Cooperative Bimetallic Effects on New Iridium(III) Pyrazolate Complexes: Hydrogen−Hydrogen, Carbon−Hydrogen, and Carbon−Chlorine Bond Activations

Eduardo Sola,[†] Vladimir I. Bakhmutov,[†,§] Francisco Torres,[†] Anabel Elduque,[†] Jose A. López,[†] Fernando J. Lahoz,[†] Helmut Werner,[‡] and Luis A. Oro*[,†]

Departamento de Química Inorgánica, Instituto de Ciencia de Materiales de Aragón, Universidad de Zaragoza, CSIC, 5009 Zaragoza, Spain, and Institut für Anorganische Chemie der Universität Würzburg, Am Hubland, D-97074 Würzburg, Germany

Received November 5, 1997

The reaction of *fac*-[$IrH_2(NCCH_3)_3(P^iPr_3)$]BF_4 (**1**) with potassium pyrazolate gave the binuclear 34-electron complex [$Ir_2(\mu\text{-H})(\mu\text{-Pz})_2H_3(NCCH_3)(P^iPr_3)_2$] (**2**). The structure of **2** was determined by X-ray diffraction. An electrostatic potential calculation located three terminal hydride ligands and one hydride bridging both iridium centers. The feasibility of this arrangement was studied by EHMO calculations. The spectroscopic data for **2** show that the complex is rigid in solution on the NMR time scale. In solution, the acetonitrile ligand of **2** dissociates. The activation parameters for this dissociation process in toluene-d_8 are $\Delta H^{\ddagger} = 20.9 \pm 0.6$ kcal mol^{-1} and $\Delta S^{\ddagger} = 2.5 \pm 1.3$ e.u. Reaction of **2** with various Lewis bases (L) gives the substitution products [$Ir_2(\mu\text{-H})(\mu\text{-Pz})_2H_3(L)(P^iPr_3)_2$] (L = C_2H_4 (**3**), CO (**4**), HPz (**5**)). The reaction of complex **5** with C_2H_4 yields the ethyl derivative [$Ir_2(\mu\text{-H})(\mu\text{-Pz})_2(C_2H_5)H_2(HPz)(P^iPr_3)_2$] (**6**); this reaction is reversible. Complexes **2** and **3** react with $CHCl_3$ to give CH_2Cl_2 and the compounds [$Ir_2(\mu\text{-H})(\mu\text{-Pz})_2H_2(Cl)(L)(P^iPr_3)_2$] (L = $NCCH_3$ (**7**), C_2H_4 (**8**)). In the ^{1}H NMR spectra of **2**−**6**, the signal of the bridging hydride ligand shows two very different J_{HP} couplings; in contrast, for the chloride complexes **7** and **8**, two equal J_{HP} couplings are observed. NOE and T_1 measurements lead to the conclusion that in complexes **2**−**6** the hydride bridges the iridium centers in a nonsymmetric fashion, whereas for **7** and **8** the bridge is symmetrical. This structural feature largely influences the reactivity. Compounds **2** and **3** undergo H/D exchange under a D_2 atmosphere. Analysis of the isotopomeric mixtures of **2** reveals downfield isotopic shifts in the $^{31}P\{^1H\}$ NMR spectrum. Downfield as well as high-field shifts are found for the hydride signals in the ^{1}H NMR spectrum of partially deuterated **2**. Further reaction of **3** with H_2 gave ethane and the dihydrogen complex [$Ir_2(\mu\text{-H})(\mu\text{-Pz})_2H_3(\eta^2\text{-}H_2)(P^iPr_3)_2$] (**9**). Under a deficiency of H_2, in toluene-d_8 solution, **9** undergoes H/D scrambling with the participation of the solvent. It has also been found that under H_2 complex **3** catalyzes the hydrogenation of cyclohexene.

Introduction

The synthesis, structure, and reactivity of binuclear metal complexes have attracted considerable interest in recent years. Originally, this interest was stimulated by using these complexes as models to study the cooperative effects between adjacent metallic centers in heterogeneous catalytic reactions.[1] The work in this area has shown the potential possibility of combining the capabilities of both metallic entities, giving rise to effective homogeneous catalytic systems.[2−6] Hence, the development of the chemistry of unsaturated binuclear complexes becomes a major goal, also in the context of homogeneous catalysis.

Inspection of representative examples of binuclear catalysts, such as [$Rh(\mu\text{-SR})(CO)(PR_3)]_2$,[2] [$Ru(\mu\text{-OAc})(CO)_2(PPh_3)]_2$,[3] *rac*-[$Rh_2(nbd)_2(et,ph\text{-}P_4)]^{2+}$,[4] or [$(CO)(PPh_3)_3HRu(\mu\text{-bim})Ir(diene)$],[6a−d] reveals the presence of low-valent, Lewis-basic mononuclear fragments. Such

* Author to whom correspondence should be addressed. E-mail: oro@posta.unizar.es.
† Instituto de Ciencia de Materiales de Aragón.
‡ Universität Würzburg.
§ Permanent address: Russian Academy of Sciences, A. N. Nesmeyanov Institute of Organo-Element Compounds, Varilov Str. 28, Moscow 117813, Russia.

(1) Collman, J. P.; Hegedus, L. S.; Norton, J. R.; Finke, R. G. *Principles and Applications of Organotransition Metal Chemistry*; University Science Books: Mill Valley, CA, 1987.
(2) Kalck, P. *Polyhedron* **1988**, *7*, 2441.
(3) Jenck, J.; Kalck, P.; Pinelli, E.; Siani, M.; Thorez, A. *J. Chem. Soc., Chem. Commun.* **1988**, 1428.
(4) (a) Matthews, R. C.; Howell, D. K.; Peng, W. J.; Train, S. G.; Treleaven, W. D.; Stanley, G. G. *Angew. Chem., Int. Ed. Engl.* **1996**, *35*, 2253. (b) Süss-Fink, G.; *Angew. Chem., Int. Ed. Engl.* **1994**, *33*, 67. (c) Broussard, M. E.; Juma, B.; Train, S. G.; Peng, W. J.; Laneman, S. A.; Stanley, G. G. *Science* **1993**, *260*, 1784.
(5) (a) Zhang, N.; Mann, C. M.; Shapley, P. A. *J. Am. Chem. Soc.* **1988**, *110*, 6591. (b) Choukroun, R.; Gervais, D.; Rifaï, C. *Polyhedron* **1989**, *8*, 1760. (c) Choukroun, R.; Iraqi, A.; Gervais, D.; Daran, J. C.; Jeannin, Y. *Organometallics* **1987**, *6*, 1197. (d) Choukroun, R.; Gervais, D.; Kalck, P.; Senocq, F. *J. Organomet. Chem.* **1987**, *335*, C9. (e) Ojima, I.; Okabe, M.; Kato, K.; Kwon, H. B.; Horváth, I. T. *J. Am. Chem. Soc.* **1988**, *110*, 150.

S0276-7333(97)00972-2 CCC: $15.00
Publication on Web 01/30/1998

metallic centers offer an excellent opportunity for the activation of organic substrates, as extensively shown for mononuclear complexes.[7] Nevertheless, the activation of organic molecules can also be effected by high-valent electrophilic metal centers. The σ-bond metathesis mechanism is the commonly proposed reaction pathway for these activations,[8−10] although in the case of late transition metals the oxidative-addition−reductive-elimination sequence cannot be definitively excluded.[11−13] This has been proven for some iridium(III) complexes, which are active in important reactions such as aliphatic C−H bond cleavage.[12−14] Unfortunately, the use of these capabilities in a catalytic cycle still remains unresolved.

Binuclear rhodium and iridium complexes with two *cis*-pyrazolate bridging ligands have been thoroughly investigated, confirming a marked flexibility of the $M_2(\mu\text{-Pz})_2$ framework.[15,16] We have recently shown that the use of strong σ-donor ligands such as CN^{t}Bu lead to very basic binuclear complexes capable of activating C−Cl bonds.[17] As an alternative approach to the design of catalytic systems, we were interested in the synthesis of coordinatively unsaturated binuclear Ir(III) complexes. Such species may display the substrate activation capabilities shown by electrophilic metal centers but extended by the cooperative advantages of bimetallic systems. This work describes a new pyrazolate-bridged diiridium system which can perform H−H, C−H, and C−Cl bond activations. In addition, this system catalyzes alkene hydrogenation.

Results

Synthesis and Characterization of the Complexes. Following our interest in the reactivity of cationic $[Ir(COD)(NCR)(PR_3)]^+$ [18] complexes, we have now observed that $[Ir(COD)(NCCH_3)(P^iPr_3)]BF_4$ reacts with dihydrogen, in acetone and in the presence of an excess of acetonitrile, leading to the formation of cyclooctene and the complex *fac*-$[IrH_2(NCCH_3)_3(P^iPr_3)]BF_4$ (**1**) in good yield. Analytical and spectroscopic data for **1** support the proposed structure with a *fac* arrangement of the acetonitrile ligands. The ^{1}H NMR spectrum displays a high-field doublet (δ −22.93, J_{HP} = 21.2 Hz) for the two equivalent hydrides *cis* to the phosphine. At low field, the spectrum shows a doublet of doublets for the phosphine methyl groups, a doublet (J_{HP} = 0.9 Hz) corresponding to the acetonitrile located *trans* to the phosphine, and a singlet due to the other two equivalent $NCCH_3$ ligands. A complex analogous to **1** with triphenylphosphine instead of P^iPr_3 has been previously described as a result of the reductive elimination of pentamethylcyclopentadiene from $[Ir(Cp^*)H_3(PPh_3)]BF_4$ in the presence of acetonitrile.[19] This complex has been assumed to have a *fac* arrangement of the acetonitrile ligands, although the spectroscopic data can be also interpreted in terms of a *mer* isomer with mutually *trans*-disposed hydrides. The $^{13}C\{^1H\}$ NMR spectrum of **1** in $CDCl_3$ shows two different signals for the quaternary carbons of the acetonitrile ligands: a singlet at δ 118.87 and a doublet with a J_{CP} = 16.9 Hz at δ 118.61. The latter, assigned to the $NCCH_3$ ligand *trans* to the phosphine, does not change under *off-resonance* conditions, whereas the singlet splits into a multiplet corresponding to the X part of an ABMX spin system (A, B = ^{1}H, M = ^{31}P). Simulation of this signal gives a J_{HH} value of 4.8 Hz for the hydride ligands and a J_{CH} value of 7.6 Hz, in agreement with a *trans* disposition of the acetonitriles and hydrides, actually confirming the *fac* arrangement.

The reaction of compound **1** with a solution of potassium pyrazolate leads to the binuclear complex $[Ir_2(\mu\text{-H})(\mu\text{-Pz})_2H_3(NCCH_3)(P^iPr_3)_2]$ (**2**), which has been characterized by elemental analysis, IR and NMR spectroscopies, and X-ray diffraction. Figure 1 shows the molecular diagram of the structure of **2**; selected bond distances and angles are listed in Table 1. Due to the low quality of the diffraction data (see Experimental Section) and to the well-known problem of the localization of hydrogens in the presence of heavy-metal centers, the four hydride ligands of **2** could not be definitively located in the X-ray analysis and have been placed in the positions estimated with the HYDEX program.[20]

Complex **2** is an asymmetric species, where only one of the iridium centers, Ir(1), possesses an acetonitrile ligand. The bridging pyrazolate units adopt the usual *cis* arrangement,[15,16] whereas the phosphines are dis-

(6) (a) Esteruelas, M. A.; García, M. P.; López, A. M.; Oro, L. A. *Organometallics* **1991**, *10*, 127. (b) García, M. P.; López, A. M.; Esteruelas, M. A.; Lahoz, F. J.; Oro, L. A. *J. Chem. Soc., Dalton Trans.* **1990**, 3465. (c) García, M. P.; López, A. M.; Esteruelas, M. A.; Lahoz, F. J.; Oro, L. A. *J. Organomet. Chem.* **1990**, *388*, 365. (d) García, M. P.; López, A. M.; Esteruelas, M. A.; Lahoz, F. J.; Oro, L. A. *J. Chem. Soc., Chem. Commun.* **1988**, 793. (e) Claver, C.; Kalck, P.; Rydmy, M.; Thorez, A.; Oro, L. A.; Pinillos, M. T.; Apreda, M. C.; Cano, F. H.; Foces-Foces, C. *J. Chem. Soc., Dalton Trans.* **1988**, 1523. (f) Kalck, P.; Thorez, A.; Pinillos, M. T.; Oro, L. A. *J. Mol. Catal.* **1985**, *31*, 311.

(7) For some recent literature reviewing activation reactions and catalytic applications of low-valent transition-metal complexes, see: (a) Schneider, J. J. *Angew. Chem., Int. Ed. Engl.* **1996**, *35*, 1068. (b) Arndtsen, B. A.; Bergman, R. G.; Mobley, T. A.; Peterson, T. H. *Acc. Chem. Res.* **1995**, *28*, 154. (c) *J. Organomet. Chem.* **1995**, *504*, 1−155. (d) Simpson, M. C.; Cole-Hamilton, D. J. *Coord. Chem. Rev.* **1996**, *155*, 163. (e) Murahashi, S. I.; Naota, T. *Bull. Chem. Soc. Jpn.* **1996**, *69*, 1805. (f) Haarman, H. F.; Ernsting, J. M.; Kranenburg, M.; Kooijman, H.; Veldman, N.; Speck, A. L.; van Leeuwen, P. W. N. M.; Vrieze, K. *Organometallics* **1997**, *16*, 887 and references therein.

(8) (a) Crellin, K. C.; Beauchamp, J. L.; Geribaldi, S.; Decouzon, M. *Organometallics* **1996**, *15*, 5368. (b) Huang, Y.; Hill, Y. D.; Sodupe, M.; Bauschlider, C. W., Jr.; Freiser, B. S. *J. Am. Chem. Soc.* **1992**, *114*, 9106. (c) Thompson, M. E.; Baxter, S. M.; Bulls, A. R.; Burger, B. J.; Nolan, M. C.; Santarsiero, B. D.; Schaefer, W. P.; Bercaw, J. E. *J. Am. Chem. Soc.* **1987**, *109*, 203.

(9) Christ, C. S.; Eyler, J. R.; Richardson, D. E. *J. Am. Chem. Soc.* **1988**, *110*, 4038.

(10) Bryndza, H. E.; Fong, L. K.; Paciello, R. A.; Tam, W.; Bercaw, J. E. *J. Am. Chem. Soc.* **1987**, *109*, 1444.

(11) Siegbahn, P. E. M.; Crabtree, R. H. *J. Am. Chem. Soc.* **1996**, *118*, 4442.

(12) Hinderling, C.; Plattner, D. A.; Chen, P. *Angew. Chem., Int. Ed. Engl.* **1997**, *36*, 243.

(13) Gutierrez, E.; Monge, A.; Nicasio, M. C.; Poveda, M.; Carmona, E. *J. Am. Chem. Soc.* **1994**, *116*, 791.

(14) (a) Luecke, H. F.; Arndtsen, B. A.; Burger, P.; Bergman, R. G. *J. Am. Chem. Soc.* **1996**, *118*, 2517. (b) Arndtsen, B. A.; Bergman, R. G. *Science* **1995**, *270*, 1970. (c) Lohrenz, J. C. W.; Jacobsen, H. *Angew. Chem., Int. Ed. Engl.* **1996**, *35*, 1305.

(15) Tejel, C.; Villoro, J. M.; Ciriano, M. A.; López, J. A.; Eguizábal, E.; Lahoz, F. J.; Bakhmutov, V. I.; Oro, L. A. *Organometallics* **1996**, *15*, 2967, and ref. therein.

(16) (a) Sadimenko, A. P.; Basson, S. S. *Coord. Chem. Rev.* **1996**, *147*, 247. (b) Trofimenko, S. *Chem. Rev.* **1993**, *93*, 943. (c) Trofimenko, S. *Prog. Inorg. Chem.* **1986**, *34*, 115.

(17) (a) Tejel, C.; Ciriano, M. A.; Oro, L. A.; Tiripicchio, A.; Ugozzoli, F. *Organometallics* **1994**, *13*, 4153. (b) Ciriano, M. A.; Tena, M. A.; Oro, L. A. *J. Chem. Soc., Dalton Trans.* **1992**, 2123.

(18) (a) Cabeza, J. A.; Cativiela, C.; Díaz deVillegas, M. D.; Oro, L. A. *J. Chem. Soc., Perkin. Trans.* **1988**, 1881. (b) Oro, L. A.; Cabeza, J. A.; Cativiela, C.; Díaz deVillegas, M. D.; Meléndez, E. *J. Chem. Soc. Chem. Commun.* **1983**, 1383.

(19) Pedersen, A.; Tilset, M. *Organometallics* **1993**, *12*, 3064.

(20) Orpen, A. G. *J. Chem. Soc., Dalton Trans.* **1980**, 2509.

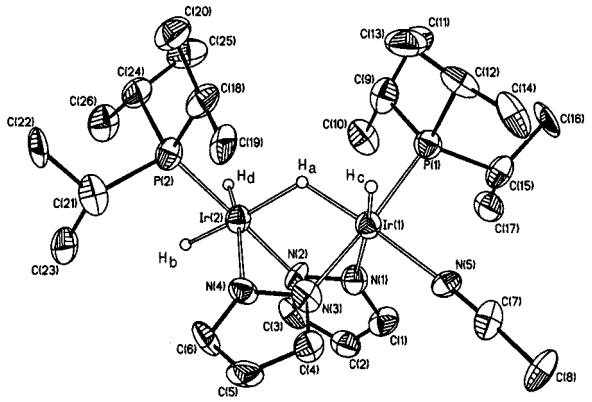

Figure 1. Molecular structure of the complex $[Ir_2(\mu\text{-H})(\mu\text{-Pz})_2H_3(NCCH_3)(P^iPr_3)_2]$ (**2**). Hydride ligands have been placed by electrostatic potential calculations.

Table 1. Selected Bond Lengths (Å) and Angles (deg) for 2[a]

Ir(1)···Ir(2)	2.9817(14)		
Ir(1)−P(1)	2.252(6)	Ir(2)−P(2)	2.216(6)
Ir(1)−N(1)	2.12(2)	Ir(2)−N(2)	2.08(2)
Ir(1)−N(3)	2.08(2)	Ir(2)−N(4)	2.10(2)
Ir(1)−N(5)	2.04(2)		
P(1)−Ir(1)−N(1)	102.0(5)	P(2)−Ir(2)−N(2)	178.1(5)
P(1)−Ir(1)−N(3)	173.1(5)	P(2)−Ir(2)−N(4)	95.9(5)
P(1)−Ir(1)−N(5)	96.0(5)	N(2)−Ir(2)−N(4)	85.3(7)
N(1)−Ir(1)−N(3)	84.2(6)	N(3)−Ir(1)−N(5)	86.7(7)
Ha−Ir(1)−Hc	91	Ha−Ir(2)−Hb	168
		Ha−Ir(2)−Hd	105
		Hc−Ir(2)−Hb	63
P(1)−Ir(1)−Ha	88	P(2)−Ir(2)−+Ha	92
P(1)−Ir(1)−Hc	87	P(2)−Ir(2)−Hb	91
N(1)−Ir(1)−Ha	88	P(2)−Ir(2)−Hd	92
N(1)−Ir(1)−Hc	171	N(2)−Ir(2)−Ha	89
N(3)−Ir(1)−Ha	89	N(2)−Ir(2)−Hb	87
N(3)−Ir(1)−Hc	86	N(2)−Ir(2)−Hd	87
N(5)−Ir(1)−Ha	176	N(4)−Ir(2)−Ha	88
N(5)−Ir(1)−Hc	89	N(4)−Ir(2)−Hb	103
Ir(1)−Ha−Ir(2)	122	N(4)−Ir(2)−Hd	167

[a] Bond angles involving calculated hydrides are included to define the metal coordination polyhedra.

posed in a *transoid* fashion occupying sites trans to the pyrazolate nitrogens (angles 173.1(5)° and 178.1(5)°). Placing the hydride ligands in their calculated positions leads to an almost regular octahedral environment for both iridium centers. The hydride H_a bridges the iridium atoms which are separated by 2.9817(14) Å. This intermetallic distance is quite long compared with typical values of Ir−Ir bond lengths,[21] although the existence of a metal−metal bond has been proposed for iridium complexes with longer intermetallic distances.[22,23]

To check the plausibility of the structure derived from this analysis, in particular the computation of the hydride positions, an extended Hückel molecular orbital calculation (EHMO)[24] has been performed. The results show a large HOMO−LUMO gap of about 2.5 eV,

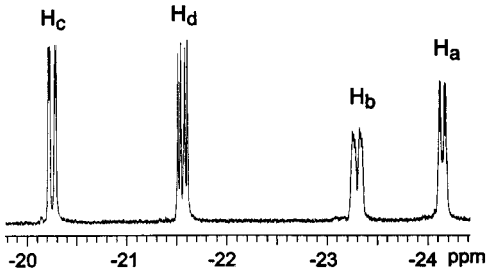

Figure 2. High-field region of the ^1H NMR spectrum of complex **2** (293 K, C_6D_6).

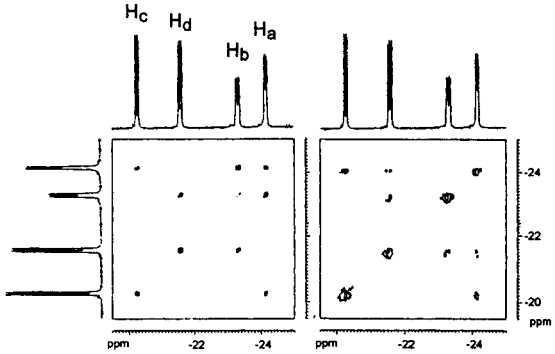

Figure 3. High-field region of the ^1H COSY (left) and NOESY (right) spectra of **2**.

confirming that the structure shown in Figure 1 constitutes a reasonable proposal, from the point of view of the electronic requirements also. The stabilization of this formally unsaturated 34-electron binuclear compound is achieved by the formation of a hydride bridge, giving rise to a three-center−two-electron bond. Analysis of the Mulliken populations between the metal centers give a small positive value (+0.018) in agreement with the existence of a weak bonding interaction.

The spectroscopic data obtained for **2** confirm that the solid-state structure is maintained in solution. The high-field region of the ^1H NMR spectrum in C_6D_6 displays four multiplets corresponding to four unequivalent hydride ligands (Figure 2). The assignments of these signals to the positions found in the structural analysis can be done with the help of the COSY and NOESY experiments outlined in Figure 3. The diagrams reveal the coupling of the bridging hydride H_a with H_c and the *trans*-located H_b and the existence of NOE effect[25] between H_a and hydrides H_c and H_d. The corresponding J_{HH} and J_{HP} coupling constants involved in those multiplets have been obtained from a $^1H\{^{31}P\}$ spectrum and ^1H double-resonance experiments and can be found in the Experimental Section. Among these NMR parameters, those concerning the bridging hydride ligand H_a will be discussed below. The other NMR parameters obtained for this complex are those expected from the solid-state structure and deserve no further comments.

The IR spectrum of complex **2** in Nujol shows two strong bands at 2183 and 2150 cm^{-1}, attributable to terminal ν(Ir−H) vibrations. Another strong band at 1724 cm^{-1} can be assigned to the stretching of the bridging hydride.[26]

In solution, the acetonitrile ligand of **2** undergoes rapid exchange with $NCCD_3$ to give $[Ir_2(\mu\text{-H})(\mu\text{-Pz})_2H_3$-

(21) The mean Ir−Ir distance for complexes where an Ir−Ir bond is proposed is 2.770 Å: 3D Search and Research using the Cambridge Structural Database. Allen, F. H.; Kennard, O. *Chem. Des. Auto. News* **1993**, *8* (1), 31.

(22) Sutherland, B. R.; Cowie, M. *Organometallics* **1985**, *4*, 1801.

(23) Kolel-Veetil, M. K.; Rheingold, A. L.; Ahmed, K. J. *Organometallics* **1993**, *12*, 3439.

(24) (a) Hoffmann, R. *J. Chem. Phys.* **1963**, *39*, 1397. (b) Hoffmann, R.; Lipscomb, W. N. *J. Chem. Phys.* **1962**, *36*, 2179. (c) Hoffmann, R.; Lipscomb, W. N. *J. Chem. Phys.* **1962**, *37*, 2872.

(25) Noggle, J.; Schirmer, R. E. *NOE*; Academic Press, Inc.: New York, 1971.

Table 2. Rate Constants for Acetonitrile Dissociation from Complex 2[a]

T (K)	[$NCCH_3$] (M)	k_{obs} (s^{-1})
283	0.2	8.6×10^{-4} [b]
283	0.4	1.07×10^{-3} [b]
283	0.8	1.37×10^{-3} [b]
283	1	1.59×10^{-3} [b]
293	0.8	5.56×10^{-3} [b]
333	0.8	0.42[c]
343	0.8	1.09[c]
353	0.8	3.1[c]

[a] [**2**] = 0.02 M. [b] By $NCCH_3/NCCD_3$ exchange. [c] By spin-saturation transfer.

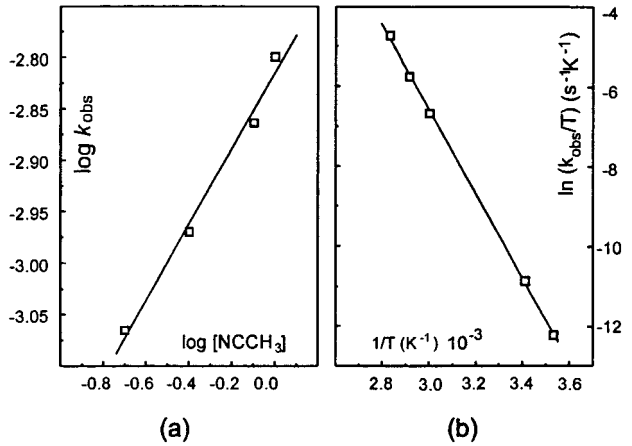

Figure 4. Kinetics of acetonitrile exchange in complex **2**. (a) Logarithmic plot of the dependence of k_{obs} *vs* acetonitrile concentration. (b) Eyring plot of the rate constants (k_{obs}) of this process.

($NCCD_3$)(P^iPr_3)$_2$] (**2**-d_3). Despite the formal electronic deficiency of complex **2**, the lack of free coordination sites and the results of the EHMO calculations suggest that this exchange most probably involves initial dissociation of acetonitrile. The kinetics of the substitution process leading to **2**-d_3 were measured in toluene-d_8 at 283 K at different $NCCD_3$ concentrations, leading to the pseudo-first-order rate constants (k_{obs}) summarized in Table 2. The logarithmic representation of Figure 4a shows a slight dependence of the experimental rate constants with respect to the acetonitrile-d_3 concentration. However, the reaction order obtained for acetonitrile is close to zero (0.37). At temperatures above 333 K, the spin-saturation-transfer method[27] permits the determination of the rate for the exchange between free and coordinated acetonitrile. Thus, it is possible to measure the rate constants for a rather broad range of temperatures and to estimate the activation parameters. The Eyring plot shown in Figure 4b gives the values $\Delta H^{\ddagger} = 20.9 \pm 0.6$ kcal mol^{-1} and $\Delta S^{\ddagger} = 2.5 \pm 1.3$ e.u. The entropy value close to zero strongly supports a monomolecular mechanism involving the dissociation of the acetonitrile ligand of complex **2**. The small dependence of the rate on the concentration of acetonitrile is most probably related to the change in the solvent properties induced by the increase of the concentration of $NCCD_3$ rather than to a real kinetic order.

Substitution of the acetonitrile ligand in **2** can be also effected by other Lewis bases, such as ethylene, CO, or pyrazole, leading to the formation of the complexes [$Ir_2(\mu$-H)(μ-Pz)$_2$H$_3$(C_2H_4)(P^iPr_3)$_2$] (**3**), [$Ir_2(\mu$-H)(μ-Pz)$_2$H$_3$-(CO)(P^iPr_3)$_2$] (**4**), and [$Ir_2(\mu$-H)(μ-Pz)$_2$H$_3$(HPz)(P^iPr_3)$_2$] (**5**), respectively. The spectroscopic data obtained for these species (Table 3 lists some of them), indicate that all of these species have structural features similar to complex **2**.

Complex **3** is readily formed after bubbling ethylene through a solution of **2** in toluene. This reaction is irreversible. The ^{1}H NMR spectrum of **3** at room temperature shows the presence of a fast spinning ethylene ligand which gives rise to a typical AA′BB′ pattern. In agreement with this, the $^{13}C\{^1H\}$ NMR spectrum displays a singlet at δ 49.21. The absence of H−P coupling for this signal supports its assignment to an η^2-C_2H_4 ligand coordinated *cis* to the phosphine. The coordination of the ethylene causes a strong downfield shift of the H_c and H_a resonances, due to the π-acceptor character of the ligand. The IR spectrum of **3** in Nujol contains a band at 1570 cm^{-1} attributable to the ν(C═C) stretching frequency.

Complex **4** can be prepared by reaction of complex **2** and CO. In the $^{13}C\{^1H\}$ NMR spectrum of **4**, the carbonyl ligand gives rise to a doublet at δ 170.68 with $J_{CP} = 7.6$ Hz, in agreement with its position *cis* to the phosphine ligand. In addition, the IR spectrum displays a strong absorption at 2025 cm^{-1}, as expected for a terminal CO group.

Complex **5** can be prepared by addition of a stoichiometric amount of pyrazole to a solution of **2** in toluene. The spectroscopic data obtained for **5** are consistent with the structure depicted in Scheme 1. The hydride ligands of **5** show ^{1}H NMR parameters very similar to those observed for **2**. In addition, the proton spectrum contains three resonances due to the ring protons of the coordinated pyrazole together with a broad resonance at δ 10.5 assigned to the N−H proton. The latter also causes a characteristic N−H stretching mode at 3404 cm^{-1} in the IR spectrum.

Bubbling ethylene through a solution of **5** leads to the formation of the ethyl complex [$Ir_2(\mu$-H)(μ-Pz)$_2$(C_2H_5)-H_2(P^iPr_3)$_2$] (**6**). Interestingly, this is a reversible process, and thus, **5** can be regenerated by removal of ethylene under an argon stream. The spectroscopic data obtained for **6** confirm the structure shown in Scheme 1. In the ^{1}H NMR spectrum, the ethyl ligand gives rise to a ABM_3X spin system (X = ^{31}P) with δ_A 2.49, δ_B 2.98, and δ_M 1.82 and the coupling constants $J_{AB} = 11.4$ Hz, $J_{AM} = J_{BM} = 7.5$ Hz, $J_{AX} = 3.7$ Hz, and $J_{BX} = 2.8$ Hz. In the $^{13}C\{^1H\}$ NMR spectrum, a doublet at δ −19.82 (J_{CP} = 6.5 Hz) and a singlet at δ 23.01 can be assigned to the carbon atoms of the ethyl group, in agreement with its *cis* position to the phosphine ligand. The high-field region of the proton spectrum displays three different signals. The resonance at highest field, which shows J_{HP} couplings of 15.3 and 5.1 Hz, is attributable to the bridging hydride H_a, while the other two resonances are assigned to the terminal hydride ligands. In the $^{31}P\{^1H\}$ NMR spectrum, two singlets appear at δ 9.52 and

(26) Gross, C. L.; Wilson, S. R.; Girolami, G. S. *J. Am. Chem. Soc.* **1994**, *116*, 10294.

(27) (a) Faller, J. W. *Determination of Organic Structures by Physical Methods*; Nachod, F. C., Zuckerman, J. J., Eds.; Academic Press: New York and London, 1973. (b) Sanders, J. K. M.; Hunter, B. K. *Modern NMR Spectroscopy, A Guide for Chemists*, 2nd ed.; Oxford University Press: New York, 1993.

Table 3. H−P and H−H Coupling Constants of the ^{1}H NMR Hydride Signals of Complexes 2−8

complex	H_a-P^1	H_a-P^2	H_b-P^2	H_c-P^1	H_d-P^2	H_a-H_b	H_a-H_c	H_a-H_d	H_b-H_d
2	15.0	3.9	21.0	19.2	19.5	3.9	3.9		8.1
3	24.0	2.4	21.1	17.4	19.2	8.4			7.8
4	13.5	4.5	21.3	16.2	20.1	8.0	2.1		8.0
5	12.3	4.0	21.6	19.2	19.8	4.0	4.0		8.4
6	15.3	5.1		19.5	23.4		4.2		
7	10.1	10.1		18.3	19.5		2.2	2.2	
8	9.6	9.6		16.5	17.7		2.4		

Scheme 1

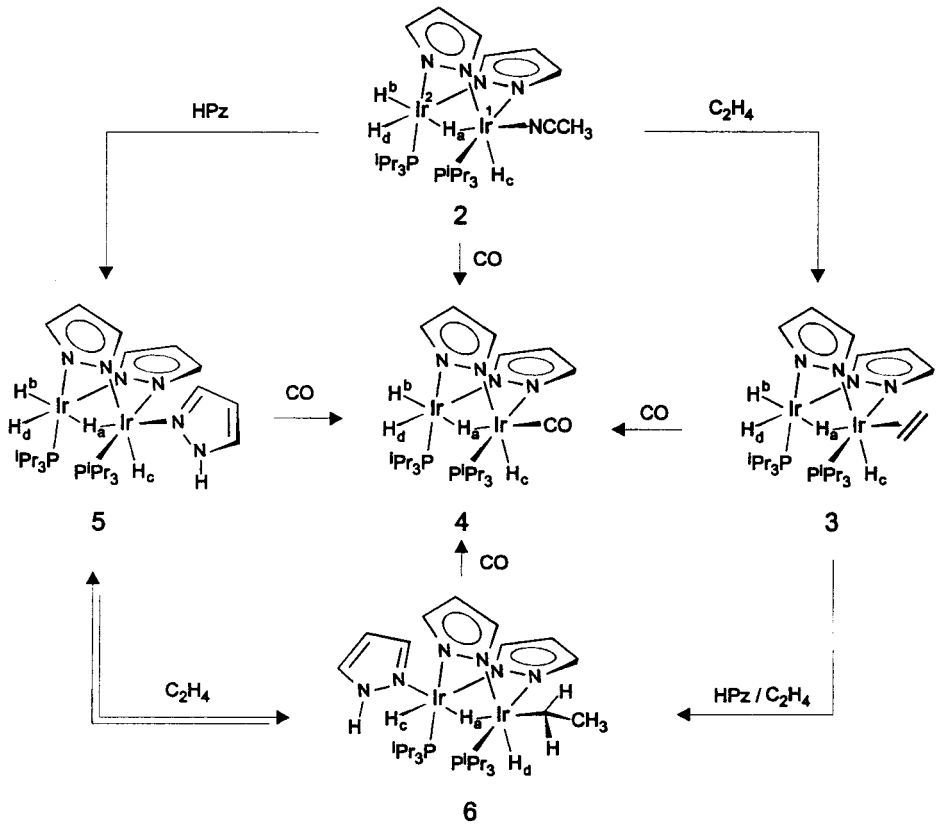

9.73, which under *off-resonance* conditions split into two doublets of doublets. This confirms the presence of one terminal hydride on each metal center. NOE experiments[25] permit one to deduce a *cis* position of the bridging hydride with respect to both terminal hydride ligands.

Complex **2** reacts with $CDCl_3$ leading to $CHDCl_2$ and the trihydride complex $[Ir_2(\mu\text{-H})(\mu\text{-Pz})_2H_2(Cl)(NCCH_3)(P^iPr_3)_2]$ (**7**). Although this reaction is slow at room temperature, complex **7** can be obtained in high yield by refluxing a solution of complex **2** in $CHCl_3$ for 5 min (Scheme 2).

The high-field region of the ^{1}H NMR spectrum of **7** shows three different hydride signals: a triplet of triplets, attributable to a bridging hydride ligand H_a, and two doublets of doublets for the two terminal hydrides H_c and H_d. Remarkably, for this complex, the signal of the bridging hydride shows identical H−P coupling constants with both phosphorus nuclei (10.1 Hz) and also the same coupling with both terminal hydrides (2.2 Hz), suggesting that H_a bridges both metal centers (see next section) symmetrically. These NMR parameters, together with the observation of two doublets of doublets in the ^{31}P *off-resonance* spectrum, allow the formulation of the structure shown in Scheme 2,

Scheme 2

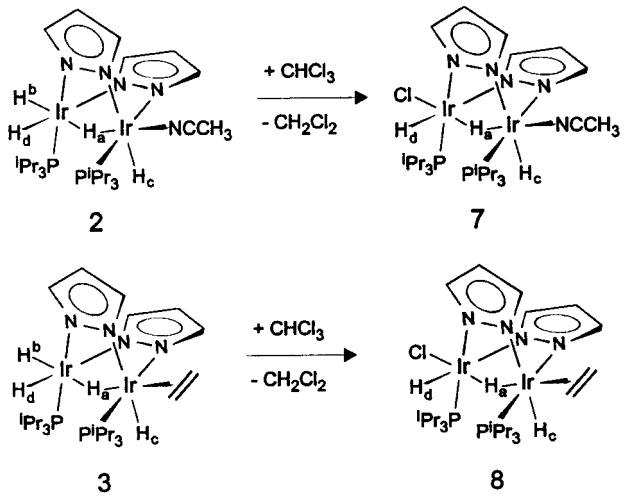

where the acetonitrile and chloride ligands are located in *trans* positions to the bridging hydride.

Complex **3** reacts with chloroform in a similar way with chloroform to give the corresponding trihydride derivative $[Ir_2(\mu\text{-H})(\mu\text{-Pz})_2H_2(Cl)(C_2H_4)(P^iPr_3)_2]$ (**8**) (Scheme 2). It is noteworthy that the related carbonyl compound **4** does not react with $CDCl_3$ under the same

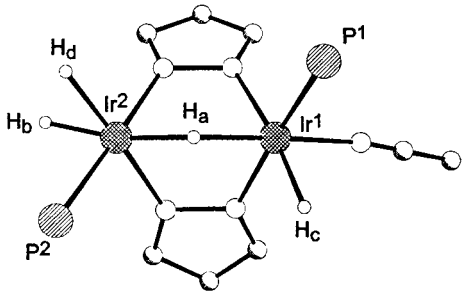

Figure 5. Schematic representation of the central core of complex $[Ir_2(\mu\text{-H})(\mu\text{-Pz})_2H_3(NCCH_3)(P^iPr_3)_2]$ (**2**).

experimental conditions. The spectroscopic data obtained for **8** are in full agreement with the proposed structure. The bridging hydride ligand H_a shows the same J_{HP} coupling with both phosphorus atoms (9.6 Hz), although it is coupled with only one of the terminal hydrides. At room temperature, the coordinated ethylene molecule displays signals very similar to the AA′BB′ pattern found for complex **3**. However, in this case, the signals are broadened, most probably due to the slow rotation of the olefin on the NMR time scale. This observation is confirmed by the presence of a broad signal at δ 45.41 in the $^{13}C\{^1H\}$ spectrum assigned to both ethylene carbon atoms.

NOE and T_1 Relaxation Studies of the Hydride Complexes. The electrostatic potential calculations (HYDEX) on the X-ray structure of **2** presented above locate the bridging hydride ligand H_a between the iridium centers, in a position geometrically equivalent with respect to both phosphorus atoms, as shown in Figure 5. However, the ^1H NMR spectrum of **2** shows remarkably different J_{HP} coupling constants of 15.0 and 3.9 Hz for the resonance of the bridging hydride H_a. The larger H−P coupling, corresponding to the P^iPr_3 ligand at Ir^1, suggests a structure in which H_a is more strongly bonded to Ir^1 than to Ir^2. This is also in accordance with the relatively small J_{HH} coupling between H_a and the *trans*-located hydride H_b (3.9 Hz) and with the absence of a H_a-H_d coupling. The presence of an asymmetric bridging hydride can also be assumed by inspection of the proton spectra of complexes **3**−**6** (Table 3). Unfortunately, a definitive assignment of the symmetric or asymmetric nature of the bridge could not be established by the above solid-state studies of **2**.

To support the asymmetric coordination of the bridging hydride H_a inferred from the NMR coupling constants, we have estimated the hydride−hydride distances in **2** by means of room-temperature NOE experiments[25] and variable-temperature T_1 measurements[28] for a solution of **2** in toluene-d_8. T_1 measurements have often been used to obtain quantitative structural information about transition-metal hydride systems.[29] It has been shown that in the case of Ir complexes,[29b,c] intramolecular dipole−dipole proton−proton interactions dominate the T_1 relaxation time of the hydride ligands. Application of the common methodology for these determinations (see Experimental Section) requires isotropic molecular reorientations.[28] Of course, this is difficult to expect for the bimetallic systems studied in this work. In fact, Figure 6 clearly shows that the CH_3 relaxation in the P^iPr_3 ligands of **2** does not go through a minimum when T_1 of the hydride ligands is minimal (263 K). A similar effect is observed for the relaxation of the CH_3 protons of the CH_3CN ligand, which reveals a minimum of T_1 (0.61 s) already at 273 K. However, it has been found recently that, for classical hydride complexes, T_{1min} remains to be a very reliable parameter for the determination of the metal−hydride or hydride−hydride distances despite the anisotropic motions.[29c,30] In this context, the T_1 times of all the hydride ligands of **2** reach minimal values at the same temperature (Figure 6), demonstrating a single correlation time for these ligands. This is also observed for the hydrides in complexes **3** and **7** (Table 4).

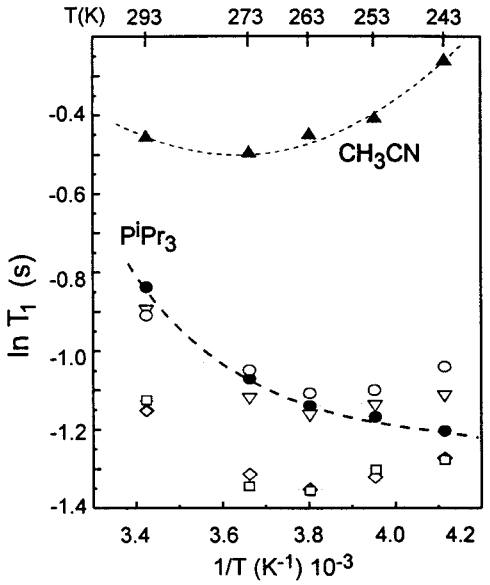

Figure 6. Variable-temperature T_1 data collected for complex **2**. The T_1 times for the hydrides are given by △, ○, ◇, and ▲, □, and and ● represent the T_1 times for the acetonitrile and phosphine methyl groups, respectively.

For complex **2**, we have observed more pronounced positive NOE enhancements (f(H)) for the H_c/H_a pair (f(H) = 0.20) than for the hydrides H_a/H_d (f(H) = 0.12). These f(H) magnitudes and the T_1 times in Table 4 were used to estimate the $r(H_a-H_c)$ and $r(H_a-H_d)$ distances as 2.38(0.05) and 2.54(0.05) Å, respectively. Thus the NOE and T_1 data confirm the suggested asymmetry of the H_a binding.

In contrast to **2**, the bridging hydride in complex **7** shows the same H−P coupling with both phosphorus atoms, suggesting a symmetric binding of H_a to both Ir centers. In agreement with this proposal, irradiation of H_c or H_d leads to very similar $f(H_a)$ values (0.08 and 0.07). Finally, in the case of complex **6,** significant NOE enhancements are observed only for the H_c/H_a pair (f(H) = 0.09). This again supports a structure with a nonsymmetrical H_a bridge.

(28) Abragam, A. *The Principles of Nuclear Magnetism*; Oxford University; New York, 1971.

(29) For example: (a) Farrar, T. C.; Quinting, G. R. *J. Phys. Chem.* **1986**, *90*, 2834. (b) Desrosiers, P. J.; Cai, L.; Lin, Z.; Richards, R.; Halpern, H. *J. Am. Chem. Soc.* **1991**, *113*, 4173. (c) Gusev, D. G.; Nietlispach, D.; Vymenits, A. B.; Bakhmutov, V. I.; Berke, H. *Inorg. Chem.* **1993**, *32*, 3270. (d) Gusev, D. G.; Vymenits, A. S.; Bakhmutov, V. I. *Inorg. Chim. Acta* **1991**, *179*, 195.

(30) To check this procedure, we have measured T_1 times for the central protons of the pyrazolate ligands, showing a minimum of 1.23 s at 263 K. This value gives a separation of 2.61 (0.05) Å between the central and lateral protons of pyrazolate, which corresponds well to that obtained from X-ray data of 2.52 Å.

Table 4. Room-Temperature T_1 and T_{1min} Data Measured for the Hydride Ligands in Complexes 2, 3, and 7 in Toluene-d_8 Solutions at 300 MHz[a]

	T_1 (s), T_{1min} (δ ppm)			
compound	H_a	H_b	H_c	H_d
2	0.320, **0.256** (−24.258)	0.402, **0.330** (−23.703)	0.409, **0.313** (−20.383)	0.316, **0.259** (−21.750)
3	0.514, **0.235** (−12.577)	0.682, **0.319** (−22.351)	0.454, **0.200** (−16.599)	0.530, **0.252** (−21.133)
7	0.244, **0.213** (−31.947)	0.365, **0.311** (−20.367)	0.348, **0.285** (−21.858)	

[a] It follows from the reproducibility of the relaxation data that a 5% experimental error should be taken into account for T_1 measurements.

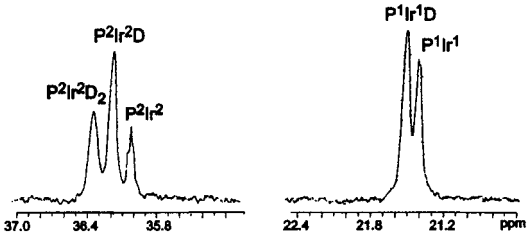

Figure 7. $^{31}P\{^1H\}$ signals of complex **2** in toluene-d_8 at 57% deuteration.

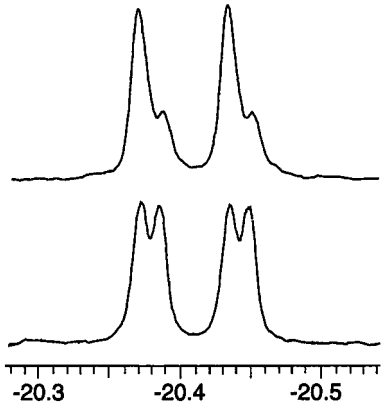

Figure 8. H_c resonance of complex **2** in toluene-d_8 before (below) and after (above) partial deuteration.

For complexes **2**, **6**, and **7**, the quantitative NOE results correspond well with the position of the H_a bridge suggested by the $J(H_a-P)$ couplings. Then, it seems reasonable to propose that, in this type of complexes, the symmetry of the bridging hydride ligand qualitatively correlates with the difference between the two $J(H_a-P)$ couplings. On the basis of this assumption and the data in Table 3, the tetrahydride complexes **3**, **4**, and **5** would contain nonsymmetric bridging arrangements whereas the chloride derivative **8** is expected to have a symmetric H_a bridge.

Deuteration of the Hydride Positions in Complex 2. Upon bubbling D_2 through a solution of **2** in toluene-d_8, the room-temperature ^1H NMR spectrum shows progressive incorporation of deuterium in all the hydride positions of the complex. This reaction is accompanied by the appearance of the resonances for uncoordinated H_2 and HD. No preferable position for deuterium was found from integral intensities of the hydride signals.

The room-temperature $^{31}P\{^1H\}$ NMR spectrum of the solution at 57% deuteration of the hydride positions is shown in Figure 7. The observed pattern can be rationalized in terms of significant downfield isotopic perturbations of ^{31}P chemical shifts upon deuteration of the terminal hydride ligands and of an unresolved influence of the D/H replacement in the H bridging position. In this context, the isotopic effect ($\Delta\delta$) is equal to 0.094 and 0.164 ppm per D for the $P^iPr_3-Ir^1$ and $P^iPr_3-Ir^2$ groups, respectively. Note that these values differ significantly, probably reflecting different electronic densities on the metal centers. It should also be noted that the above $\Delta\delta$ values are larger in magnitude with regard to the isotopic effect reported for *cis*-$[IrCl_2H(H_2)(PiPr_3)_2]$.[31]

The room-temperature ^1H NMR spectrum of partially deuterated (57%) complex **2** shows some interesting features. The spectrum exhibits complicated resonance patterns for the hydride ligands because of the presence of an isotopomeric mixture. Despite this, a *low-field* shift of 0.012 ppm is determined for H_c (Figure 8), illustrating the influence of the D/H exchange at the bridging hydride position. A similar isotopic shift (+0.0145 ppm) is clearly deduced from the pattern of the H_d signal if the terminal H_b position is occupied by D, as follows from the disappearance of the H_d-H_b coupling.

Downfield isotopic perturbations have already been reported for various transition-metal hydride systems.[31−35] In the case of the tris(pyrazolyl)borate complexes $[IrH(Tp)(H_2)(PMe_3)]BF_4$[33] and $[IrH_4(Tp^*)]$,[32] the large temperature-dependent downfield shifts were interpreted in terms of dihydrogen/hydride exchange and classical nonrigid hydride structures, respectively. Complex **2** is a classical and rigid (on the NMR time scale) polyhydride in the solid state and in solution (see the T_1 data in Table 4). Thus, it can be assumed that the observed downfield isotopic shifts represent an *intrinsic* phenomenon for complex **2** instead. Moreover, for this compound we have found a high-field shift of −0.009 ppm, observed for the signal of H_d after deuteration at the bridging hydride position. It is interesting that this isotopic effect is lower in magnitude and opposite in sign to that observed for H_c after deuteration at the same bridging position. We believe that this observation can be correlated with the nonsymmetrical arrangement of H_a between the two iridium centers of complex **2**.

(31) Albinati, A.; Bakhmutov, V. Y.; Caulton, K. G.; Clot, E.; Eckert, J.; Eisenstein, O.; Gusev, D. G.; Grushin, V. V.; Hauger, B. E.; Klooster, W. T.; Koetzle, T. F.; McMillan, R. K.; Oloughlin, T. J.; Peliussier, M.; Ricci, J. S.; Sigalas, M. P.; Vymenits, A. B. *J. Am. Chem. Soc.* **1993**, *115*, 7300.

(32) Paneque, M.; Poveda, M. L.; Taboada, S. *J. Am. Chem. Soc.* **1994**, *116*, 4519.

(33) Heinekey, D. M.; Oldham, W. J. *J. Am. Chem. Soc.* **1994**, *116*, 3137.

(34) Nanz, D.; Vonphilipsborn, W.; Bucher, U. E.; Venanzi, L. M. *Magn. Reson. Chem.* **1991**, *29*, S38.

(35) Michos, D.; Luo, X.-L.; Crabtree, R. H. *Inorg. Chem.* **1992**, *31*, 4245.

Scheme 3

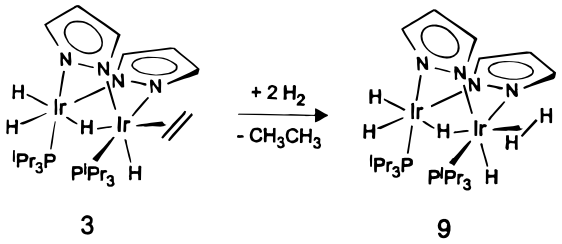

A correct determination of the isotopic shifts for H_b and H_a was unsuccessful due to the complex character of their resonances. Nevertheless, in the case of H_a, it is clear that one of the observed effects is quite large (+0.0645 ppm). Finally, it should be noted that no H−D coupling was resolved in the ^{1}H NMR spectrum, as expected for a classical polyhydride.[36]

Preparation and NMR Studies of a Binuclear η^2-H_2 Complex. Bubbling H_2 through a solution of complex **3** in toluene-d_8 leads to the formation of a new complex **9** and ethane. The reaction is very slow at room temperature but becomes fast upon heating to 313 K under a H_2 atmosphere (due to the low solubility of H_2 in toluene, only 1 mg of **3** was taken for the experiments). It is important to note that no free ethylene was observed in the ^{1}H NMR spectrum, in contrast to the behavior found for the non-hydride complex [Ir(Tp)(C_2H_4)(PPh_3)] that gives free ethylene upon treatment with H_2.[37]

The hydride region of the room-temperature ^{1}H NMR spectrum of the product solution showed almost complete disappearance of the starting material **3** and the appearance of a new broad triplet at δ −13.72 with a small J_{HP} constant of 6.6 Hz. Irradiation of the single resonance at δ 27.94 observed in the ^{31}P{^{1}H} NMR spectrum leads to a transformation of the triplet hydride signal to a singlet. The protons of the pyrazolate ligands of the new complex **9** give rise to three resonances at δ 5.87, 7.25, and 7.34 in the integral ratio of 1:1:1. In turn, the signal of the hydride ligands shows a 3-fold integral intensity with respect to each line of the pyrazolate units. The T_{1min} time of the hydride resonance is 0.054 s (300 MHz, 233 K), significantly shorter than the values found for the starting complex **3** (Table 4). This T_{1min} suggests that **9** can be formulated (Scheme 3) as a nonclassical polyhydride, where the hydride ligands undergo fast hydride/hydride and dihydrogen/hydride exchange on the NMR time scale.[36]

The variable-temperature ^{1}H NMR spectra, recorded for a solution of **9** in toluene-d_8 (for comparison in the presence of complex **3**, see Figure 9), show a typical exchange evolution. The hydride resonance at δ −13.72 undergoes a broadening effect at 233 K, disappears at 193 K, and appears again at 163 K as four broadened signals at δ −9.71, −11.28, −19.81, and −22.09, respectively, with an integral intensity ratio of 3:1:1:1. Note that a similar ^{1}H NMR temperature behavior was reported earlier, for example, for complex [($Ptol_3$)(H_2)-Ru(μ-H)(μ-Cl)$_2$RuH($Ptol_3$)].[38a]

The low-temperature ^{1}H NMR spectrum of **9** presented in Figure 9 illustrates that the hydride/hydride exchange is slow on the NMR time scale while the H_c/(H_2) is still quite fast. The latter has often been observed for dihydrogen complexes with *cis* arrangements of the H and H_2 ligands.[31,39,40] For example, in the case of the iridium complex [Ir(Tp)H(H_2)(PMe_3)]BF_4, the activation energy for the H/H_2 exchange was estimated to be 5 kcal mol^{-1}.[32] The spectra in Figure 9 correlate well with the appearance of two lines at δ 32.8 and 22.6 in the 163 K ^{31}P{^{1}H} NMR spectrum. These resonances are also broadened due to the hydride/hydride exchange. The rate constant of this exchange can be estimated from the line width of the ^{31}P{^{1}H} signals[41] by using the line width of complex **3** as a reference. This calculation gives a k value of 470 s^{-1} ($\Delta G^{\ddagger}$(−105° C) = 7.8 kcal mol^{-1}). A similar energy barrier (7.6 kcal mol^{-1}) can be calculated from the line widths of the signals of the hydride ligands in the 163 K ^{1}H NMR spectrum of **9**. Possible mechanisms of the H/H and H/(H_2) exchange in bimetallic dihydrogen complexes have already been discussed.[38e]

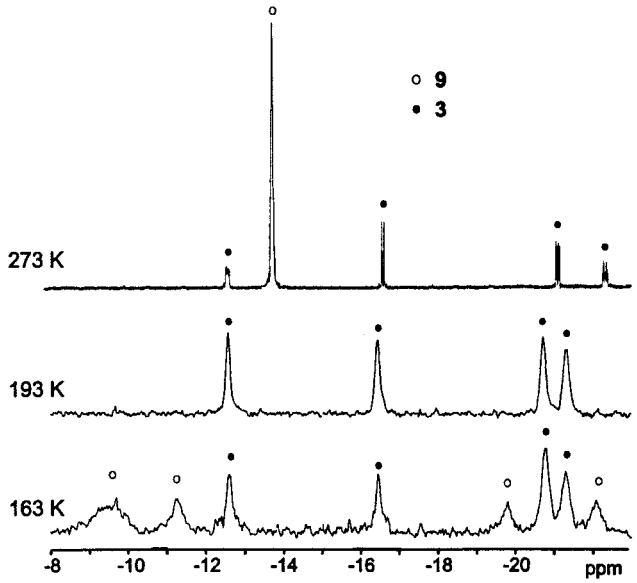

Figure 9. High-field region of the variable-temperature ^{1}H NMR spectra of complex **9** (in the presence of complex **3**) in toluene-d_8.

The T_{1min} time allows an estimation of the H−H distance[36] in the dihydrogen ligand of **9**. Under the conditions of the fast hydride/hydride exchange, the T_{1min} of 0.054 s corresponds to 0.021 s for the dihydrogen ligand. The contribution to the relaxation rate of the (H_2) ligand, caused by dipole−dipole interactions with the P^iPr_3 and pyrazolate groups, can be estimated as 1/0.251 s^{-1}, where 0.251 s represents an averaged T_{1min} time observed for the signal of the hydride ligands in complexes **2** and **3** (see Table 4). The T_{1min} time of 0.0229 s, calculated for the (H_2) ligand, gives a r(H−H)

(36) (a) Jessop, P. G.; Morris, R. H. *Coord. Chem. Rev.* **1992**, *121*, 155. (b) Heinekey, D. M.; Oldham, W. J. *Chem. Rev.* **1993**, *93*, 913.
(37) Oldham, W. J.; Heinekey, D. M. *Organometallics* **1997**, *16*, 467.
(38) (a) Hampton, C.; Dekleva, T. W.; James, B. R.; Cullen, W. R. *Inorg. Chim. Acta* **1988**, *145*, 165. (b) Hampton, C.; Cullen, W. R.; James, B. R. *J. Am. Chem. Soc.* **1988**, *110*, 6918. (c) Joshi, A. M.; James, B. R. *J. Chem. Soc. Chem. Commun.* **1989**, 1785. (d) He, Z.; Nefedov, S.; Lugan, N.; Neibecker, D.; Mathieu, R. *Organometallics* **1993**, *12*, 3837. (e) Hampton, C.; Butler, I. R.; Cullen, W. R.; James, B. R.; Charland, J.-P.; Simpson, J. *Inorg. Chem.* **1992**, *31*, 5509.
(39) Bakhmutov, V. I.; Vymenits, A. B.; Grushin, V. V. *Inorg. Chem.* **1994**, *33*, 4413.
(40) Bianchini, C.; Linn, K.; Masi, D.; Peruzzini, M.; Polo, A.; Vacca, A.; Zanobini, F. *Inorg. Chem.* **1993**, *32*, 2366.
(41) Jackman, L. N.; Cotton, F. A *Dynamic Nuclear Magnetic Resonance Spectroscopy*; Academic Press: New York, 1975; p 45.

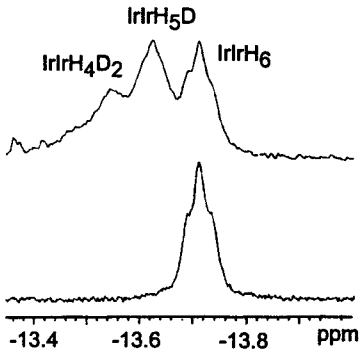

Figure 10. High-field signal of the ^{1}H NMR spectrum of **9** in toluene-d_8 at 293 K before (below) and after (above) partial deuteration.

distance equal to 1.20 or 0.95 Å in the slow- or fast-rotation limits,[36] respectively. Note, that a quantitative interpretation of the T_1 data in such cases still remains open to discussion.[36,42]

It has recently been found that the rate of H_2 loss from mononuclear iridium−dihydrogen complexes correlates with the elongation of the H−H bond in the (H_2) ligand.[43] Taking this observation into account, we have examined the ^{1}H NMR spectra of complex **9** in the presence of excess of H_2, finding a very pronounced saturation-transfer effect[27] at 313 K. The hydride resonance of **9** loses 36% of the integral intensity upon irradiation of the resonance of free H_2. In turn, this corresponds to the rate of H_2 loss of 7.6 s^{-1}. In our opinion, these data definitely support the formulation of **9** as a dihydrogen complex. Moreover, it should be mentioned that *cis*-[$IrCl_2H(H_2)(P^iPr_3)_2$], with the elongated (H−H) bond (1.11 Å, neutron diffraction), eliminates H_2 very slowly even at 353 K.[31]

Finally, we note that, unfortunately, the arrangement of the dihydrogen ligand with respect to the bridging hydride H_a in **9** remains unclear. However, if we take into consideration that *trans* arrangements of H_a and L have been found for all the compounds obtained from **2**, we believe that the (H_2) ligand in compound **9** is also located *trans* to the hydride H_a. Such a *trans* position of H_2 and hydride has also been established for the mononuclear tetrahydrides [$IrXH_2(H_2)(PR_3)_2$].[44]

Deuteration Reactions of the Dihydrogen Complex 9. Treatment of the ethylene complex **3** with D_2 in a toluene-d_8 solution at room temperature (a lack of D_2 was used for simultaneous observation of the resonances of **3** and **9**) results in deuterium incorporation at the hydride positions of **9**. Figure 10 shows the signals due to complex **9** after a reaction time of 15 min. No deuteration of complex **3** is detected at this stage.

The three lines in Figure 10 can definitely be assigned to $IrIrH_6$, $IrIrH_5D$, and $IrIrH_4D_2$ isotopomers with large downfield isotopic perturbations of 0.085 ppm per D. Similar data have been reported recently for partially deuterated [$Ir(Tp)H(H_2)(PMe_3)$]BF_4.[33] It follows from Figure 10 that the (H−D) coupling constants are unresolved in the ^{1}H NMR spectrum at 293 K. Nevertheless, the expected broadening effects are clearly observed for the resonances of the isotopomers. Upon standing in solution for 5 h, the ^{1}H NMR spectrum indicates the formation of an $IrIrH_3D_3$ isotopomer of **9** with an isotope shift of 0.067 ppm. Interestingly, deuterium is now detected in the ethylene ligand and in the hydride positions of complex **3**.

Identical experiments were carried out with a deficiency of H_2 instead of D_2. In this case, the ^{1}H NMR spectrum of the solution confirms the presence of complex **9** containing 25% of the $IrIrH_5D$ isotopomer. It seems to be obvious that deuteration of the dihydrogen complex **9**, obtained from **3** and H_2, is due to D/H exchange by the participation of toluene-d_8. We assume that the latter is coordinated on the Ir center after dissociation of the dihydrogen ligand. In agreement with this, we have found that the exchange is practically blocked (on the same reaction time scale) in the presence of an excess of H_2. A rather similar exchange between the hydride ligands and deuterated solvents has recently been reported for the unsaturated complex [$IrClH_2(P^iPr_3)_2$] also.[44]

Scheme 4

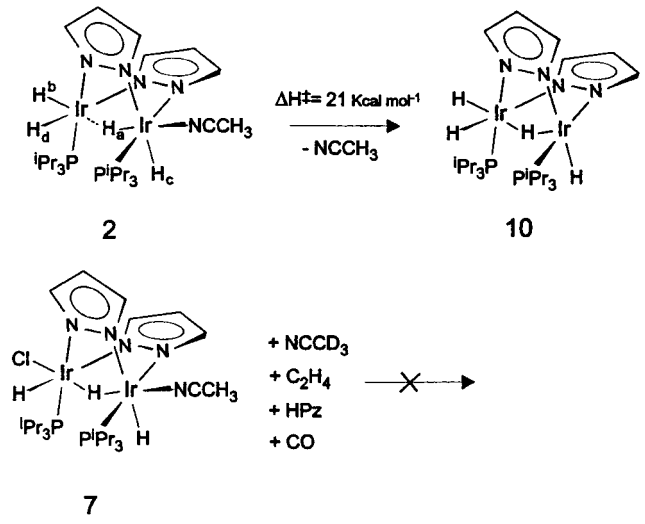

Discussion

The present investigations have shown that the new pyrazolate-bridged diiridium complex **2** exhibits a high reactivity in substitution reactions and is also capable to perform H−H, C−H, and C−Cl bond activations. The chemical behavior of this bimetallic system clearly illustrates that the reactivity of one metal center strongly depends on the ligand environment of the second metal atom, despite the long Ir−Ir distance and the weak bonding interaction.

This finding could be rationalized by taking into account the structural features of this system. The spectroscopic studies of complex **2** confirm the presence of a hydride ligand bridging both metallic centers in a nonsymmetric fashion (Scheme 4). In contrast, the structure deduced for the chloride derivative **7** contains a symmetrically bridging hydride.

The structural difference between **2** and **7** (and also between **3** and **8**) can easily be correlated with the different *trans* influence[45] of the chloride and hydride ligands. The asymmetric position of the bridging hydride in **2** is rationalized as a result of the large *trans*

(42) Gusev, D. G.; Kuhlman, R. L.; Renkema, K. B.; Eisenstein, O.; Caulton, K. G. *Inorg. Chem.* **1996**, *35*, 6775.
(43) Bakhmutov, V. I.; Vorontsov, V. V.; Vymenits, A. B. *Inorg. Chem.* **1995**, *34*, 214.

influence of the hydride H_b. Therefore, the relatively low activation energy for the dissociation of the acetonitrile ligand from **2** ($\Delta H^{\ddagger} = 20.9 \pm 0.6$ kcal mol^{-1} in toluene-d_8) reflects the large *trans* effect provoked by the nonsymmetric hydride bridge. In contrast to complex **2**, the acetonitrile ligand of **7** *trans* to the symmetrically bridging H_a is not replaced in the presence of pyrazole, CO, or ethylene. Consequently, the above observations can be interpreted as the transmission of a *trans* influence through the binuclear framework, via the bridging hydride, giving rise to a *binuclear trans effect*. This interpretation is also in agreement with the molecular orbital scheme calculated for **2**, which shows a strong mixing of the σ orbitals of the $H_b-Ir-H_a-Ir-NCCH_3$ backbone. This could permit the transmission of a *trans* effect due to a pure σ-bonding ligand[45] from one extreme of the molecule to the other.

The high reactivity found for complex **2** compared with the inert behavior of **7** clearly indicates that the reactivity of this type of binuclear species depends on the capability of the saturated precursor to create a vacant coordination site (an associative mechanism does not seem to be operating). From this point of view, the already described reactivity would be understood in terms of the characteristics of the generated unsaturated intermediates. In this respect, there are two important observations to be considered: first, these species are able to undergo intermolecular reactions, and therefore, the lifetime of the intermediates should be long enough to undergo intramolecular rearrangements. Second, the reaction products of the intermolecular reactions reveal a complete regioselectivity. These observations allow the conclusion that, despite the fast intramolecular rearrangement processes, only one state has an appropriate lifetime to react. In favor of this proposal, it should be noted that a small energy barrier has been determined for the hydride−hydride exchange in the nonclassical complex **9**. It has also been shown that intramolecular rearrangements in metal polyhydrides are frequently fast processes in solution[36] and in the solid state.[46]

Indeed, the factors influencing the stereochemistry of the intermediates should be related to those determining the structure of the stable products. From the above discussion, we know that the *trans* influence of ligands is an important factor to understand the structural features of these binuclear polyhydrides. Moreover, the configuration of the reaction intermediates proposed below lead us to assume that the large *trans* influence of hydride ligands would favor the formation of species with the free coordination site *trans* to hydride.

Most of the chemistry described in the previous section can be understood as a result of the reactivity of the already formulated intermediate **10** (Scheme 4). This species can react directly with different Lewis bases to give the substitution products shown in Scheme 1.

$$\mathbf{2} \rightleftarrows NCCH_3 + \mathbf{10} \xrightarrow{L} \mathbf{3}, \mathbf{4}, \mathbf{5}$$

Scheme 5

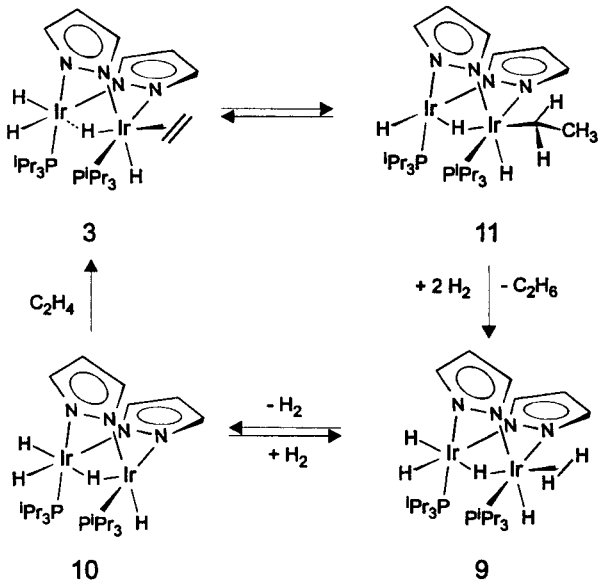

In solutions of complex **2**, the lifetime of intermediate **10** is long enough to allow a reaction with D_2 and $CDCl_3$, leading to products of H/D and H/Cl exchange, respectively. Possible mechanisms for these reactions have already been discussed.[7f,47] For the activation of X−H bonds, an initial coordination of this σ-bond with the metal center has been proposed.[47] In this respect, deuteration of complex **2** under D_2 most probably involves the formation of the dihydrogen species **9** in nondetectable concentrations. In agreement with this, very low energy barriers have been estimated for the hydride/hydride and hydride/dihydrogen exchange within the bimetallic framework of **9** (see Results section).

The dihydrogen compound **9** could not be detected during the treatment of **2** with H_2, which can be attributed to the stronger bonding capabilities of acetonitrile with respect to dihydrogen. This thermodynamic preference for acetonitrile is reflected in the rate of ligand dissociation from the binuclear unit. Thus, dissociation of H_2 from **9** is much faster (7.6 s^{-1} at 313 K) than the corresponding release of acetonitrile from complex **2** (0.06 s^{-1} at 313 K). A similar thermodynamic situation may be expected for the intermediates involved in the H/Cl metathesis reactions. The structure of complex **7** resulting from this reaction suggests that an intramolecular rearrangement of the hydride ligands occurs after H/Cl exchange, directing the coordination of the incoming acetonitrile to the position *trans* to the bridging hydride.

The formation of the ethyl complex **6** suggests that the dissociation step to give intermediate **10** is not the preferred pathway for the activation of **3**. Instead, the structure of **6** allows the formulation of **11** (Scheme 5) as the most probable reactive species generated from **3**. This species may result from the insertion of ethylene into a *cis* Ir−H[48] bond followed by hydride migration. The reversibility of the formation of **6** from **5** seems to indicate that this species can undergo a β-elimination to yield ethylene. This is also in agree-

(44) Mediati, M.; Tachibana, G. N.; Jensen, C. M. *Inorg. Chem.* **1992**, *31*, 1827.
(45) Armstrong, D. R.; Fortune, R.; Perkins, P. G. *Inorg. Chim. Acta* **1974**, *9*, 9 and references therein.
(46) Wisniewski, L. L.; Mediati, M.; Jensen, C. M.; Zilm, K. W. *J. Am. Chem. Soc.* **199**3, *115*, 7533.
(47) Crabtree, R. H. *Angew. Chem., Int. Ed. Engl.* **1993**, *32*, 789.

ment with the formation of compound **4** by treatment of **6** or **3** with CO (Scheme 1).

Intermediate **11** can react in a similar way to **10**, as evidenced by the reaction of **3** with $CHCl_3$ to give complex **8** and by the occurrence of H/D exchange of **3** in the presence of D_2. Interestingly, under a D_2 atmosphere, incorporation of deuterium into the ethylene ligand occurs as soon as H/D exchange in the hydride positions of **3** is detected. This is in full agreement with the existence of an insertion/β-elimination process involving intermediate **11**.[48] In this context, it should be noted that in some mononuclear complexes a hydride/α-CH_2 exchange has been shown to take place faster that the elimination of an alkane.[47]

The elimination of ethane from **3** in the presence of H_2 provides a simple way to quantitatively generate complex **9**. This reaction requires heating of the reaction mixture at 313 K for a few minutes. It should be mentioned that a similar synthetic strategy was recently employed to obtain the ruthenium polyhydride [Ru(Tp)H$(H_2)_2$].[49] Although a few examples of bimetallic dihydrogen complexes have been reported in the literature,[36b,38] to the best of our knowledge complex **9** is the first binuclear Ir/Ir species containing a molecular dihydrogen ligand.

It has been shown frequently that dihydrogen complexes constitute a convenient way to stabilize temporarily unsaturated species in solution, due to the easy dissociation of the H_2 ligand.[36] Therefore, **9** can be seen, in the presence of hydrogen and in the absence of better coordinating ligands, as the stabilized form of intermediate **10**. In fact, solutions of **9** afford complex **3** upon treatment with ethylene (Scheme 5). This reaction closes a cycle for ethylene hydrogenation, suggesting that complex **3** can be used as a precursor for the catalytic hydrogenation of alkenes via the unsaturated species **10**. In accordance with this result, the catalytic hydrogenation of cyclohexene can be performed at room temperature and atmospheric H_2 pressure using **3** as a catalyst precursor. The reaction requires preactivation by heating a solution of **3** at 313 K for a few minutes, in agreement with the experimental conditions found for the generation of the dihydrogen complex **9**.

Removal of the excess H_2 from the solutions of **9** in toluene-d_8 results in the occurrence of H/D exchange with the participation of the solvent. This observation reveals that, under conditions favoring an appropriate lifetime of the intermediate **10**, this species activates C−H bonds, in analogy to other well-known mononuclear Ir(III) systems.[12−14]

In the view of the capabilities of intermediate **10** to activate different types of σ bonds such as C−H, C−Cl, and H−H, we have briefly examined the interaction of the acetonitrile complex **2** with Et_3SiH. No visible changes were found in the room-temperature ^{1}H NMR spectrum of a toluene-d_8 solution of **2** in the presence of an excess of Et_3SiH. However, under the same conditions, the partially deuterated complex **2** clearly undergoes H/D exchange with the silane. This result is consistent with the reactivity already described for compound **10** and with the possibility of reversible coordination of the Si−H bond to the five-coordinate iridium center of **10** in an η^2-fashion.[50]

Conclusion

This work describes the preparation and reactivity of new binuclear iridium(III) complexes containing the "Ir(μ-H)(μ-Pz)$_2$Ir" framework, which are able to activate H−H, C−H, and C−Cl bonds. The studies performed revealed a *remarkable bimetallic character* of this system, taking into account that the reactivity of one metal center strongly depends on the ligand environment of the second metal atom. This behavior results from the transmission of a *trans* effect from one metallic fragment to the other, via the bridging hydride ligand.

This system has also provided the first example of a diiridium complex containing a coordinated dihydrogen molecule [$Ir_2(\mu$-H)(μ-Pz)$_2H_3(\eta^2$-$H_2)(P^iPr_3)_2$] (**9**). This dihydrogen complex is most probably involved in the cycle of the alkene hydrogenation catalyzed by the complex [$Ir_2(\mu$-H)(μ-Pz)$_2H_3(C_2H_4)(P^iPr_3)_2$] (**3**).

Experimental Section

Physical Measurements. Infrared spectra were recorded as Nujol mulls on polyethylene sheets using a Nicolet 550 spectrometer. C, H, N analyses were carried out in a Perkin-Elmer 2400 CHNS/O analyzer. NMR spectra were recorded on a Varian Unity, a Varian Gemini 2000, or a Bruker ARX 300 MHz spectrometer. The temperature was calibrated by ^{1}H NMR with a standard methanol sample. ^{1}H and ^{13}C chemical shifts were measured relative to partially deuterated solvent peaks but are reported in parts per million (ppm) relative to tetramethylsilane. ^{31}P chemical shifts were measured relative to H_3PO_4 (85%). Coupling constants are given in hertz. Generally, spectral assignments were achieved by ^{1}H COSY and NOESY and ^{13}C DEPT experiments. The relaxation times T_1 were obtained by a conventional inversion−recovery method. The calculations of the relaxation times were made using the fitting routine of the Varian spectrometers. A 5% experimental error for T_1 measurements follows from the reproducibility of the relaxation experiments.

Synthesis. All reactions were carried out with the exclusion of air by using standard Schlenk techniques. Solvents were dried by known procedures and distilled under argon prior to use. The complex [Ir(COD)$(NCCH_3)(P^iPr_3)$]BF_4 was prepared following a general procedure described in ref 51.

Preparation of *fac*-[$IrH_2(NCCH_3)_3(P^iPr_3)$]BF_4 (1). A solution of [Ir(COD)$(NCCH_3)(P^iPr_3)$]BF_4 (200 mg, 0.34 mmol) in 5 mL of CH_2Cl_2 was treated with 500 μL of acetonitrile, and the mixture was stirred under dihydrogen at atmospheric pressure for 2 h. The resulting yellow solution was concentrated to ca. 0.5 mL, and diethyl ether was added to give a white solid. The solvent was decanted, and the solid was washed several times with diethyl ether and dried in vacuo: yield 167 mg (88%); IR (Nujol mull, cm^{-1}) 2260, 2265 (s, ν(Ir−H)), 1100 (br, BF_4); ^{1}H NMR ($CDCl_3$, 293 K) δ −22.93 (d, J_{HP} = 21.2, 2H, Ir−H), 1.10 (dd, J_{HP} = 14.0, J_{HH} = 6.5, 18H, PCHCH_3), 2.04 (m, 6H, PCHCH_3), 2.36 (s, 6H, NCCH_3), 2.40 (d, J_{HP} = 0.9, 3H, NCCH_3); ^{31}P{^{1}H} NMR ($CDCl_3$, 293 K) δ 30.35 (s); ^{13}C{^{1}H} NMR ($CDCl_3$, 293 K) δ 2.89 (s, NCCH_3), 3.12 (s, NCCH_3), 19.03 (s, PCHCH_3), 24.95 (d, J_{CP} = 34.3, PCHCH_3),

(48) (a) Lundquist, E. G.; Folting, K.; Streib, W. E.; Huffman, J. C.; Eisenstein, O.; Caulton, K. G. *J. Am. Chem. Soc.* **1990**, *112*, 855. (b) Belli, J.; Jensen, C. M. *Organometallics* **1996**, *15*, 1532. (c) Barbaro, P.; Bianchini, C.; Meli, A.; Peruzzini, M.; Vacca, A.; Vizza, F. *Organometallics* **1991**, *10*, 2227.

(49) Moreno, B.; Sabo-Etienne, S.; Chaudret, B. *J. Am. Chem. Soc.* **1994**, *116*, 2635.

(50) Luo, X. L.; Kubas, G. J.; Burns, C. J.; Bryan, J. C.; Unkefer, C. J. *J. Am. Chem. Soc.* **1995**, *117*, 1159.

(51) Crabtree, R. H.; Morris, G. E. *J. Organomet. Chem.* **1977**, *135*, 395.

118.61 (d, J_{CP} = 16.9, N*C*CH$_3$), 118.87 (s, N*C*CH$_3$). Anal. Calcd for $C_{15}H_{32}N_3BF_4PIr$: C, 31.92; H, 5.71; N, 7.44. Found: C, 31.59; H, 5.56; N, 7.18.

Preparation of [Ir$_2$(μ-H)(μ-Pz)$_2$H$_3$(NCCH$_3$)(P^{i}Pr$_3$)$_2$] (2). A solution of pyrazole (60.25 mg, 0.89 mmol) was treated with 0.9 equiv of potassium hydroxide in methanol, and the resulting mixture was added to a solution of *fac*-[IrH$_2$(NCCH$_3$)$_3$(P^{i}Pr$_3$)]BF$_4$ (**1**) (500 mg, 0.85 mmol) in 5 mL of methanol. After the mixture was stirred for 90 min, a white solid was formed, which was decanted, washed with methanol, and dried in vacuo. The solid was recrystallized by storing a saturated solution in acetone at 273 K for 2 days, giving colorless crystals: yield 247 mg (66%); IR (Nujol mull, cm^{-1}) 2183, 2150 (s, ν(Ir−H)), 1724 (s, ν(IrHIr)); ^{1}H NMR (C$_6$D$_6$, 293 K) δ −24.57 (dddd, $J_{H_aP^1}$ = 15.0, $J_{H_aH_b}$ = $J_{H_aH_c}$ = $J_{H_aP^2}$ = 3.9, 1H, H$_a$), −24.00 (dddd, $J_{H_bP^2}$ = 21.0, $J_{H_bH_d}$ = 8.1, $J_{H_bH_a}$ = $J_{H_bP^1}$ = 3.9, 1H, H$_b$), −22.18 (dd, $J_{H_dP^2}$ = 19.5, $J_{H_dH_b}$ = 8.1, 1H, H$_d$), −20.58 (dd, $J_{H_cP^1}$ = 19.2, $J_{H_cH_a}$ = 3.9, 1H, H$_c$), 1.03 (dd, J_{HP} = 14.0, J_{HH} = 7.0, 9H, PCHC*H*$_3$), 1.04 (dd, J_{HP} = 14.7, J_{HH} = 7.2, 9H, PCHC*H*$_3$), 1.13 (dd, J_{HP} = 13.4, J_{HH} = 7.2, 9H, PCHC*H*$_3$), 1.14 (dd, J_{HP} = 13.8, J_{HH} = 7.2, 9H, PCHC*H*$_3$), 1.55 (s, 3H, NCCH$_3$), 1.97, 2.27 (m, 3H each, P*C*HCH$_3$), 5.59 (dt, J_{HH} = J_{HP} = 1.5, 1H, CH$_{Pz}$), 5.93 (dt, J_{HH} = J_{HP} =1.2, 1H, CH$_{Pz}$), 7.23 (m, 1H, CH$_{Pz}$), 7.31 (m, 1H, CH$_{Pz}$), 7.37, 7.39 (d, J_{HH} = 1.8, 1H each, CH$_{Pz}$); ^{31}P{^{1}H} NMR (C$_6$D$_6$, 293 K) δ 15.86 (s), 29.16 (s); ^{13}C{^{1}H} NMR (C$_6$D$_6$, 293 K) δ 1.60 (s, NC*C*H$_3$), 18.91, 19.30, 19.48, 19.81 (s, PCH*C*H$_3$), 25.19 (d, J_{CP} = 29.4, P*C*HCH$_3$), 26.21 (d, J_{CP} = 29.9, P*C*HCH$_3$), 103.12 (d, J_{CP} = 2.8, CH$_{Pz}$), 103.45 (d, J_{CP} = 3.2, CH$_{Pz}$), 117.48 (s, N*C*CH$_3$), 134.01 (d, J_{CP} = 5.3, CH$_{Pz}$), 135.29 (d, J_{CP} = 3.4, CH$_{Pz}$), 139.11 (d, J_{CP} = 4.0, CH$_{Pz}$), 142.59 (d, J_{CP} = 5.2, CH$_{Pz}$). Anal. Calcd for $C_{26}H_{55}N_5Ir_2P_2$: C, 35.32; H, 6.27; N, 7.92. Found: C, 35.59; H, 6.22; N, 7.76.

Preparation of [Ir$_2$(μ-H)(μ-Pz)$_2$H$_3$(H$_2$C=CH$_2$)(P^{i}Pr$_3$)$_2$] (3). Ethylene was bubbled through a solution of [Ir$_2$(μ-H)(μ-Pz)$_2$H$_3$(NCCH$_3$)(P^{i}Pr$_3$)$_2$] (**2**) (150 mg, 0.17 mmol) in 5 mL of toluene for 2 min. After the mixture was stirred for 10 min, the solvent was removed in vacuo and the residue was dissolved in 3 mL of methanol. The resulting solution was filtered through kieselgur and stored at 243 K to give white crystals: yield 69 mg (47%); IR (Nujol mull, cm^{-1}) 2210, 2185, 2137 (s, ν(Ir−H)), 1722 (w, ν(IrHIr)), 1570 (s, ν(C=C)); ^{1}H NMR (C$_6$D$_6$, 293 K) δ −22.22 (ddd, $J_{H_bP^2}$ = 21.1, $J_{H_bH_a}$ = 8.4, $J_{H_bH_d}$ = 7.8, 1H, H$_b$), −21.03 (dd, $J_{H_dP^2}$ = 19.2, $J_{H_dH_b}$ = 7.8, 1H, H$_d$), −16.58 (d, $J_{H_cP^1}$ = 17.4, 1H, H$_c$), −12.55 (ddd, $J_{H_aP^1}$ = 24.0, $J_{H_aH_b}$ = 8.4, $J_{H_aP^2}$ = 2.4, 1H, H$_a$), 0.70 (dd, J_{HP} = 13.2, J_{HH} = 7.2, 9H, PCHC*H*$_3$), 0.95 (dd, J_{HP} = 13.2, J_{HH} = 6.9, 9H, PCHC*H*$_3$), 1.19 (dd, J_{HP} = 12.6, J_{HH} = 7.2, 18H, PCHC*H*$_3$), 1.90, 2.13 (m, 3H each, P*C*HCH$_3$), 3.40 (AA′BB′ system, δ_A = 3.33, δ_B = 3.47, $J_{AA'}$ = $J_{BB'}$ = 13.0, J_{AB} = $J_{A'B'}$ = 9.0, $J_{AB'}$ = $J_{A'B}$ = 0, 4H, H$_2$C=CH$_2$), 6.00 (dt, J_{HP} = J_{HH} = 2.1, 1H, CH$_{pz}$), 6.01 (dt, J_{HP} = J_{HH} = 2.1, 1H, CH$_{pz}$), 6.87 (d, J_{HH} = 2.1, 1H, CH$_{pz}$), 7.47 (m, 1H, CH$_{pz}$), 7.57 (d, J_{HH} = 1.8, 1H, CH$_{pz}$), 7.68 (m, 1H, CH$_{pz}$); ^{31}P{^{1}H} NMR (C$_6$D$_6$, 293 K) δ 0.01 (s), 31.06 (s); ^{13}C{^{1}H} NMR (C$_6$D$_6$, 293 K) δ 18.38 (d, J_{CP} = 1.9, PCH*C*H$_3$), 19.18 (d, J_{CP} = 1.4, PCH*C*H$_3$), 19.92, 20.04 (s, PCH*C*H$_3$), 25.36 (d, J_{CP} = 29.4, P*C*HCH$_3$), 25.69 (d, J_{CP} = 29.8, P*C*HCH$_3$), 49.21 (s, H$_2$C=CH$_2$), 103.75, 105.02 (s, CH$_{pz}$), 138.50 (d, J_{CP} = 3.4, CH$_{Pz}$), 140.52 (s, CH$_{pz}$), 143.95, 144.17 (d, J_{CP} = 1.2, CH$_{pz}$). Anal. Calcd for $C_{26}H_{56}N_4Ir_2P_2$: C, 35.85; H, 6.48; N, 6.43. Found: C, 35.68; H, 6.18; N, 6.14.

Preparation of [Ir$_2$(μ-H)(μ-Pz)$_2$H$_3$(CO)(P^{i}Pr$_3$)$_2$] (4). Carbon monoxide was bubbled through a solution of [Ir$_2$(μ-H)(μ-Pz)$_2$H$_3$(NCCH$_3$)(P^{i}Pr$_3$)$_2$] (**2**) (150 mg, 0.17 mmol) in 5 mL of toluene for 2 min. After the mixture was stirred for 10 min, the solvent was removed in vacuo and the residue was dissolved in 3 mL of methanol. The resulting solution was filtered through kieselgur and stored at 243 K to give white crystals: yield 78 mg (53%); IR (Nujol mull, cm^{-1}) 2178 (br, ν(Ir−H)), 2025 (s, ν(CO)); ^{1}H NMR (C$_6$D$_6$, 293 K) δ −21.74 (m, $J_{H_bP^2}$ = 21.3, $J_{H_bH_d}$ = $J_{H_bH_a}$ = 8.0, $J_{H_bH_c}$ = 1.4, $J_{H_bP^1}$ = 2.7, 1H, H$_b$), −21.66 (m, $J_{H_dP^2}$ = 20.1, $J_{H_dH_b}$ = 8.0, 1H, H$_d$), −16.70 (ddd, $J_{H_cP^1}$ = 16.2, $J_{H_cH_a}$ = 2.1, $J_{H_cH_b}$ = 1.4, 1H, H$_c$), −12.91 (dddd, $J_{H_aP^1}$ = 13.5, $J_{H_aH_b}$ = 8.0, $J_{H_aH_c}$ = 2.1, $J_{H_aP^2}$ = 4.5, 1H, H$_a$), 0.66 (dd, J_{HP} = 14.7, J_{HH} = 7.0, 9H, PCHC*H*$_3$), 0.82 (dd, J_{HP} = 14.1, J_{HH} = 7.2, 9H, PCHC*H*$_3$), 0.96 (dd, J_{HP} = 12.6, J_{HH} = 6.9, 9H, PCHC*H*$_3$), 1.01 (dd, J_{HP} = 12.9, J_{HH} = 7.2, 9H, PCHC*H*$_3$), 1.87, 2.05 (m, 3H each, PC*H*CH$_3$), 5.78 (dt, J_{HP} = J_{HH} = 2.1, 1H, CH$_{pz}$), 5.85 (dt, J_{HP} = J_{HH} = 1.8, 1H, CH$_{pz}$), 7.19 (d, J_{HH} = 1.8, 1H, CH$_{pz}$), 7.30 (m, 1H, CH$_{pz}$), 7.35 (d, J_{HH} = 2.1, 1H, CH$_{pz}$), 7.53 (m, 1H, CH$_{pz}$); ^{31}P NMR (C$_6$D$_6$, 293 K) δ 19.73 (s), 31.15 (s); ^{13}C{^{1}H} NMR (C$_6$D$_6$, 293 K) δ 18.81 (d, J_{CP} = 1.4, PCH*C*H$_3$), 19.12 (d, J_{CP} = 1.9, PCH*C*H$_3$), 19.60, 20.07 (s, PCH*C*H$_3$), 25.78 (d, J_{CP} = 29.8, P*C*HCH$_3$), 26.96 (d, J_{CP} = 31.7, P*C*HCH$_3$), 105.16, 105.25, 138.78 (d, J_{CP} = 3.3, CH$_{pz}$), 139.38 (d, J_{CP} = 4.3, CH$_{pz}$), 140.39 (d, J_{CP} = 4.2, CH$_{pz}$), 144.47 (d, J_{CP} = 5.2, CH$_{pz}$), 170.68 (d, J_{CP} = 7.6, Ir−CO). Anal. Calcd for $C_{25}H_{52}N_4Ir_2OP_2$: C, 34.47; H, 6.02; N, 6.43. Found: C, 35.17; H, 6.08; N, 6.09.

Preparation of [Ir$_2$(μ-H)(μ-Pz)$_2$H$_3$(HPz)(P^{i}Pr$_3$)$_2$] (5). Pyrazole (11.6 mg, 0.17 mmol) was added to a solution of [Ir$_2$(μ-H)(μ-Pz)$_2$H$_3$(NCCH$_3$)(P^{i}Pr$_3$)$_2$] (**2**) (150 mg, 0.17 mmol) in 5 mL of toluene. After the reaction mixture was stirred for 30 min, the solvent was removed in vacuo and the residue was treated with methanol to give a white solid. The solid was decanted, washed with methanol, and dried in vacuo: yield 118 mg (76%); IR (Nujol mull, cm^{-1}) 3404 (s, ν(N−H)), 2164, 2154 (s, ν(Ir−H)), 1732 (s, ν(IrHIr)); ^{1}H NMR (C$_6$D$_6$, 293 K) δ −25.04 (dddd, $J_{H_aP^1}$ = 12.3, $J_{H_aH_b}$ = $J_{H_aH_c}$ = $J_{H_aP^2}$ = 4.0, 1H, H$_a$), −23.22 (ddd, $J_{H_bP^2}$ = 21.6, $J_{H_bH_d}$ = 8.4, $J_{H_bH_a}$ = 4.0, 1H, H$_b$), −21.37 (dd, $J_{H_dP^2}$ = 19.8, $J_{H_dH_b}$ = 8.4, 1H, H$_d$), −21.00 (dd, $J_{H_cP^1}$ = 19.2, $J_{H_cH_a}$ = 4.0, 1H, H$_c$), 0.93 (dd, J_{HP} = 12.6, J_{HH} = 6.9, 9H, PCHC*H*$_3$), 1.09 (dd, J_{HP} = 13.2, J_{HH} = 7.5, 9H, PCHC*H*$_3$), 1.27 (dd, J_{HP} = 12.6, J_{HH} = 7.2, 9H, PCHC*H*$_3$), 1.31 (dd, J_{HP} = 12.9, J_{HH} = 7.2, 9H, PCHC*H*$_3$), 2.21, 2.31 (m, 3H each, PC*H*CH$_3$), 5.71 (dd, J_{HH} = 2.7, 2.1, 1H, CH$_{Pz}$), 6.17 (dt, J_{HH} = 2.1, J_{HP} = 2.1, 1H, CH$_{Pz}$), 6.22 (dt, J_{HH} = 1.8, J_{HP} =1.0, 1H, CH$_{Pz}$), 6.29 (d, J_{HH} = 2.1, 1H, CH$_{Pz}$), 6.40 (d, J_{HH} = 2.7, 1H, CH$_{Pz}$), 7.57 (dd, J_{HH} = 2.1, J_{HP} = 0.9, 1H, CH$_{Pz}$), 7.66 (d, J_{HH} = 1.8, 1H, CH$_{Pz}$), 7.77 (m, 1H, CH$_{Pz}$), 8.04 (m, 1H, CH$_{Pz}$), 10.50 (br, 1H, NH); ^{31}P{^{1}H} NMR (C$_6$D$_6$, 293 K) δ 11.64 (s), 30.91 (s); ^{13}C{^{1}H} NMR (C$_6$D$_6$, 293 K) δ 18.54, 19.82, 20.24 (s, PCH*C*H$_3$), 25.32 (d, J_{CP} = 29.2, P*C*HCH$_3$), 26.25 (d, J_{CP} = 29.9, P*C*HCH$_3$), 104.08 (d, J_{CP} = 2.4, CH$_{Pz}$), 105.11 (d, J_{CP} = 2.7, CH$_{Pz}$), 106.90 (s, CH$_{Pz}$), 129.49 (s, CH$_{Pz}$), 134.76 (d, J_{CP} = 4.7, CH$_{Pz}$), 135.51 (t, J_{CP} = 2.4, CH$_{Pz}$), 139.52 (t, J_{CP} = 5.0, CH$_{Pz}$), 144.76 (t, J_{CP} = 5.3, CH$_{Pz}$), 145.67 (d, J_{CP} = 5.3, CH$_{Pz}$). Anal. Calcd for $C_{27}H_{56}N_6Ir_2P_2$: C, 35.59; H, 6.19; N, 9.22. Found: C, 35.22; H, 6.49; N, 8.78.

Preparation of [Ir$_2$(μ-H)(μ-Pz)$_2$(CH$_2$CH$_3$)H$_2$(HPz)(P^{i}Pr$_3$)$_2$] (6). The product was prepared in an NMR tube by bubbling ethylene through a solution of [Ir$_2$(μ-H)(μ-Pz)$_2$H$_3$(HPz)(P^{i}Pr$_3$)$_2$] (**5**) in 0.5 mL of C$_6$D$_6$ for 1 min. In the presence of an excess of ethylene, **6** is the only detectable product: IR (C$_6$H$_6$, cm^{-1}) 3404 (s, ν(N−H)), 2156 (s, ν(Ir−H)), 1733(s, ν(IrHIr)); ^{1}H NMR (C$_6$D$_6$, 293 K) δ −26.63 (ddd, $J_{H_aP^1}$ = 15.3, $J_{H_aP^2}$ = 5.1, $J_{H_aH_c}$ = 4.2, 1H, H$_a$), −22.23 (d, $J_{H_dP^2}$ = 23.4, 1H, H$_d$), −21.03 (dd, $J_{H_cP^1}$ = 19.5, $J_{H_cH_a}$ = 4.2, 1H, H$_c$), 0.80 (dd, J_{HP} = 13.2, J_{HH} = 7.2, 9H, PCHC*H*$_3$), 0.98 (dd, J_{HP} = 12.6, J_{HH} = 7.2, 9H, PCHC*H*$_3$), 1.08 (dd, J_{HP} = 12.3, J_{HH} = 7.2, 9H, PCHC*H*$_3$), 1.24 (dd, J_{HP} = 12.3, J_{HH} = 6.9, 9H, PCHC*H*$_3$), 1.82 (t, J_{HH} = 7.5, 3H, CH$_3$), 2.17, 2.44 (m, 3H each, PC*H*CH$_3$), 2.49 (A part of a ABM$_3$X system (X = ^{31}P), J_{AB} = 11.4, J_{AM} = 7.5, J_{AX} = 3.7, 1H, IrCH$_2$), 2.98 (B part of a ABM$_3$X system (X = ^{31}P), J_{AB} = 11.4, J_{BM} = 7.5, J_{BX} = 2.8, 1H, IrCH$_2$), 5.62 (dd, J_{HH} = 2.7, 2.0, 1H, CH$_{Pz}$), 6.07 (d, J_{HH} = 2.0, 1H, CH$_{Pz}$), 6.08 (dt, J_{HH} = 1.8, J_{HP} = 1.5, 1H, CH$_{Pz}$), 6.31 (d, J_{HH} = 2.7, 1H, CH$_{Pz}$), 6.33 (dt, J_{HH} = J_{HP} = 1.5, 1H, CH$_{Pz}$), 7.56 (m, 1H, CH$_{Pz}$), 7.61 (d, J_{HH} = 1.5, 1H, CH$_{Pz}$), 7.99 (m, 1H, CH$_{Pz}$), 8.29 (d, J_{HH} = 1.8, 1H, CH$_{Pz}$); ^{31}P{^{1}H} NMR (C$_6$D$_6$, 293 K) δ 9.52 (s), 9.73 (s); ^{13}C{^{1}H} NMR (C$_6$D$_6$, 293 K) δ −19.82 (d, J_{CP} = 6.5, IrCH$_2$), 18.68, 18.90, 19.63 (s, PCH*C*H$_3$), 23.01 (s, CH$_3$), 26.34 (d, J_{CP} = 29.0, P*C*HCH$_3$), 26.71 (d, J_{CP} = 28.0, P*C*HCH$_3$), 103.82 (d, J_{CP} = 2.6, CH$_{Pz}$),

104.83 (d, J_{CP} = 3.4, CH_{Pz}), 106.95 (s, CH_{Pz}), 129.69 (s, CH_{Pz}), 134.79 (d, J_{CP} = 4.5, CH_{Pz}), 135.88 (dd, J_{CP} = 4.8, 3.0, CH_{Pz}), 136.56 (t, J_{CP} = 4.5, CH_{Pz}), 137.19 (t, J_{CP} = 4.0, CH_{Pz}), 145.90 (d, J_{CP} = 5.1, CH_{Pz}).

Preparation of $[Ir_2(\mu\text{-}H)(\mu\text{-}Pz)_2H_2(Cl)(NCCH_3)(P^iPr_3)_2]$ (7). A solution of $[Ir_2(\mu\text{-}H)(\mu\text{-}Pz)_2H_3(NCCH_3)(P^iPr_3)_2]$ (**2**) (150 mg, 0.17 mmol) in 5 mL of chloroform was heated for 10 min under reflux. The solvent was removed in vacuo, and the residue was treated with methanol to give a white solid, which was decanted, washed with methanol, and dried in vacuo: yield 128 mg (82%); IR (Nujol mull, cm^{-1}) 2197, 2179 (s, ν(Ir−H)), 1755 (w, ν(IrHIr)); ^1H NMR ($CDCl_3$, 293 K) δ −31.95 (dddd, $J_{H_aP^1} = J_{H_aP^2}$ = 10.1, $J_{H_aH_c} = J_{H_aH_d}$ = 2.2, 1H, H_a), −21.84 (dd, $J_{H_dP^2}$ = 19.5, $J_{H_dH_a}$ = 2.2, 1H, H_d), −20.36 (dd, $J_{H_cP^1}$ = 18.3, $J_{H_cH_a}$ = 2.2, 1H, H_c), 0.98 (dd, J_{HP} = 14.1, J_{HH} = 7.2, 9H, PCHCH_3), 0.99 (dd, J_{HP} = 14.1, J_{HH} = 6.9, 9H, PCHCH_3), 1.13 (dd, J_{HP} = 13.5, J_{HH} = 6.9, 9H, PCHCH_3), 1.15 (dd, J_{HP} = 13.5, J_{HH} = 6.9, 9H, PCHCH_3), 1.79 (s, 3H, NCCH_3), 2.28, 2.43 (m, 3H each, PCHCH_3), 5.93 (dt, J_{HH} = 1.8, J_{HP} = 1.5, 1H, CH_{Pz}), 6.00 (dt, J_{HH} = 1.8, J_{HP} =1.5, 1H, CH_{Pz}), 7.35 (d, J_{HH} = 1.8, 1H, CH_{Pz}), 7.40 (dd, J_{HH} = 1.8, J_{HP} = 0.9, 1H, CH_{Pz}), 7.71 (dd, J_{HH} = 1.8, J_{HP} = 1.2, 1H, CH_{Pz}), 7.91 (d, J_{HH} = 1.8, 1H, CH_{Pz}); $^{31}P\{^1H\}$ NMR ($CDCl_3$, 293 K) δ 5.87 (s), 9.86 (s); $^{13}C\{^1H\}$ NMR ($CDCl_3$, 293 K) δ 2.37 (s, NCCH_3), 18.59 (s, PCHCH_3), 19.67 (d, J_{CP} = 1.9, PCHCH_3), 19.79 (s, PCHCH_3), 25.88 (d, J_{CP} = 30.1, PCHCH$_3$), 26.14 (d, J_{CP} = 29.6, PCHCH$_3$), 102.89 (br, CH_{Pz}), 116.12 (s, NCCH$_3$), 132.39 (d, J_{CP} = 4.5, CH_{Pz}), 134.52 (dd, J_{CP} = 4.3, 2.8, CH_{Pz}), 135.19 (d, J_{CP} = 3.0, CH_{Pz}), 136.09 (dd, J_{CP} = 4.0, 2.3, CH_{Pz}). Anal. Calcd for $C_{26}H_{54}N_5Ir_2P_2Cl$: C, 33.99, H, 5.92, N, 7.62. Found: C, 34.27, H, 6.30, N, 7.50.

Preparation of $[Ir_2(\mu\text{-}H)(\mu\text{-}Pz)_2H_2(Cl)(H_2C{=}CH_2)(P^iPr_3)_2]$ (8). A solution of $[Ir_2(\mu\text{-}H)(\mu\text{-}Pz)_2H_3(H_2C{=}CH_2)(P^iPr_3)_2]$ (**3**) (150 mg, 0.17 mmol) in 2 mL of chloroform was heated for 10 min. under reflux. The solvent was removed in vacuo, and the residue was dissolved in methanol and stored at 233 K to give white crystals: yield 99 mg (65%); IR (Nujol mull, cm^{-1}): 2167, 2027 (s, ν(Ir−H)), 1722 (w, ν(IrHIr)); ^1H NMR ($CDCl_3$, 293 K) δ −22.98 (ddd, $J_{H_aP^1} = J_{H_aP^2}$ = 9.6, $J_{H_aH_c}$ = 2.4, 1H, H_a), −20.97 (dd, $J_{H_dP^2}$ = 17.7, $J_{H_dH_a}$ = 2.4,1H, H_d), −15.71 (d, $J_{H_cP^1}$ = 16.5, 1H, H_c), 0.91 (dd, J_{HP} = 13.5, J_{HH} = 7.2, 9H, PCHCH_3), 1.07 (dd, J_{HP} = 13.2, J_{HH} = 7.2, 9H, PCHCH_3), 1.15 (dd, J_{HP} = 14.1, J_{HH} = 6.0, 9H, PCHCH_3), 1.21 (dd, J_{HP} = 12.3, J_{HH} = 6.9, 9H, PCHCH_3), 2.18, 2.61 (m, 3H each, PCHCH$_3$), 3.58 (broad AA′BB′ system, δ_A = 3.51, δ_B = 3.63, 4H, $H_2C{=}CH_2$), 5.86 (dt, J_{HH} = 2.1, J_{HP} = 1.8, 1H, CH_{pz}), 5.95 (dt, $J_{HP} = J_{HH}$ = 1.8, 1H, CH_{pz}), 6.76 (d, J_{HH} = 2.1, 1H, CH_{pz}), 7.55 (dd, $J_{HP} = J_{HH}$ = 2.1, 1H, CH_{pz}), 7.72 (m, 1H, CH_{pz}), 8.01 (d, J_{HH} = 1.8, 1H, CH_{pz}); $^{31}P\{^1H\}$ NMR ($CDCl_3$, 293 K) δ −6.46 (s), 4.90 (s); $^{13}C\{^1H\}$ NMR ($CDCl_3$, 293 K) δ 18.53, 18.75, 19.05, 19.27 (s, PCHCH_3), 25.46 (d, J_{CP} = 29.3, PCHCH$_3$), 26.20 (d, J_{CP} = 30.0, PCHCH$_3$), 45.41 (br, $H_2C{=}CH_2$), 103.06, 104.07 (dd, J_{CP} = 2.7, 1.4, CH_{Pz}), 126.59 (d, J_{CP} = 5.3, CH_{Pz}), 134.89 (dd, J_{CP} = 5.9, 4.5, CH_{pz}), 136.64 (dd, J_{CP} = 5.5, 4.7, CH_{pz}), 137.77 (t, J_{CP} = 4.1, CH_{pz}). Anal. Calcd for $C_{26}H_{55}N_4Ir_2P_2Cl$: C, 34.48; H, 6.12; N, 6.18. Found: C, 34.74; H, 5.72; N, 6.12.

Kinetic Analysis. The kinetics of the exchange between the acetonitrile ligand of complex **2** and acetonitrile-d_3 was measured in 0.02 M toluene-d_8 solutions of **2** at 283 and 293 K. The decrease of the intensity of the acetonitrile signal of **2** was measured at intervals automatically in a Varian Gemini 2000 spectrometer. The rate constants were obtained by fitting the data to an exponential decay function, using the routine programs of the spectrometer. Above 333 K, the rate constants were measured by spin-saturation transfer according to the Forsén−Hoffman method[27a] in 0.02 M toluene-d_8 solutions of **2** containing 0.8 M acetonitrile. Experiments were performed by irradiating the resonance of the free acetonitrile and measuring the integral of the coordinated acetonitrile resonance. The exchange rates k_{obs} were calculated from the eq 1,[27b] where I' and I are the integrals for the coordinated acetonitrile resonance with and without saturation of the free acetonitrile resonance, respectively. T_1 is the spin−lattice

$$k = (1/T_1)((I/I') - 1) \quad (1)$$

relaxation time of the coordinated acetonitrile signal obtained by the inversion−recovery method in the presence of the saturating field at the free acetonitrile signal.[52] The activation parameters, $\Delta H^{\ddagger}$ and $\Delta S^{\ddagger}$, were obtained from a linear least-squares fit of $\ln(k/T)$ vs $1/T$ (Eyring equation). Errors were computed by published methods.[53] The error in temperature was assumed to be 1 K, the error in k_{obs} was estimated as 10%.

The rates for hydride/hydride exchange in complex **9** at 163 K (k) were estimated from the line width of the $^{31}P\{^1H\}$ signals of **9** (T_2^{obs}) through eq 2,[41] by using the line width of complex **3** as a reference (T_2*). The same procedure was followed for

$$1/\pi T_2^{obs} - 1/\pi T_2^* = 1/\pi\tau \text{ where } k = 1/\tau \quad (2)$$

the ^1H hydride signals.

NOE and T_1 Relaxation Studies. The relaxation contribution caused by proton−proton dipole−dipole interactions in a pair of protons can be obtained from NOE experiments through eq 3,[25] where $f^b(H_a)$ is the NOE enhancement observed for H_a at irradiation of H_b, $\rho(H_a{-}H_b)$ is the relaxation rate by H_a/H_b interactions, and $R(H_a)$ is the total relaxation rate of H_a. This equation is only valid at temperatures far above that

$$f^b(H_a) = \rho(H_a{-}H_b)/R(H_a) \quad (3)$$

of T_{1min} (narrowing region), but the calculated ratio between both relaxation rates can also be assumed to be valid at the temperature of T_{1min}. At this temperature, the total relaxation rate of H_a ($1/T_{1min}^{obs}$) can be expressed as the sum of the relaxation rate due to H_a/H_b interactions ($1/T_{1min}$) and the rate contribution caused by dipole−dipole interactions between the H_a ligand and all other protons ($1/T_{1min}$(other)) through eq 4.[28]

$$1/T_{1min}^{obs} = 1/T_{1min} + 1/T_{1min}(\text{other}) \quad (4)$$

Then, the room-temperature NOE effects, along with the measured T_{1min} times, allow the calculation of the relaxation rate due to a pair of protons $1/T_{1min}$. Then, assuming isotropic motions (see Results section), the internuclear hydride−hydride distance can be easily calculated through eq 5,[29d] where ν is the ^1H NMR resonance frequency (MHz).

$$r(H{-}H)\ (Å) = 2.405\ (200\ T_{1min}/\nu)^{1/6} \quad (5)$$

The determinations of NOE enhancements $f^b(H_a)$ were made by conventional procedures in two independent room-temperature experiments for each complex.

X-ray Crystallography. Transparent twinned plates of **2** were obtained by cooling a saturated solution of the complex in acetone. A thin plate of approximate dimensions 0.65 × 0.18 × 0.01 mm was selected and used for the data collection; a detailed ω-scan of several randomly searched reflections showed that the selected sample was not a single crystal but a twin with a principal component. Several thicker crystals, photographically tested, clearly showed more complicated twins. Despite the bad shape of some reflections, an orientation matrix was established for the principal component of the twinned crystal on the basis of 15 reflections. Diffraction data were collected with a Siemens P4 diffractometer using graphite-monochromated Mo Kα radiation (λ = 0.710 73 Å). Cell constants were obtained from the least-squares fit on the setting angles of 50 reflections in the range 15° ≤ 2θ ≤ 25°. There were 7801 reflections with 2θ in the range 4−48°

(52) Mann, B. E. *J. Magn. Reson.* **1977**, *25*, 91.
(53) Morse, P. M.; Spencer, M. O.; Wilson, S. R.; Girolami, G. S. *Organometallics* **1994**, *13*, 1646.

measured using the $\omega/2\theta$ scan technique and corrected for Lorentz and polarization effects. Due to the highly anisotropic shape of the selected crystal, an empirical absorption correction specially designed for thin plates was applied.[54a] This approach is based on the general ψ-scan method[54b] but refines only three shape factors ($\mu \cdot t$ and two edge factors). The required experimental information for this correction includes the Miller indices of the principal face of the crystal, the minimum glancing angle, and a set of ψ-scan measurements (1 0 0, 3°, and 11 ref., in our case). Merging R_{int} factors before and after the absorption correction were 0.2257 and 0.0687. Minimum and maximum transmission factors applied were 0.295 and 0.748. After the elimination of the reflections clearly affected by the second component of the twinned crystal and those almost parallel to the main face of the plate, 5862 nonunique reflections remained in the data set. Three standard reflections were measured every hour as a check of crystal and instrument stability; no important variation was observed.

The structure was solved by direct methods (SIR92)[55] and difference Fourier techniques and refined by full-matrix least-squares on F^2 (SHELXL93),[56] first with isotropic and then with anisotropic displacement parameters for the non-hydrogen atoms. The hydrogen atoms (except the hydride ligands) were introduced in calculated positions and refined riding on the corresponding carbon atoms. Several attemps to locate and refine the hydride positions were carried out, but unfortunately, the final geometrical parameters—particularily the Ir—H bond distances—appear to be unreasonable. The refinement converged at w$R(F^2) = 0.1752$ for 316 parameters, 100 restraints (applied to anisotropic displacement parameters) and 4259 unique reflections used in the refinement, from a total of 5638 before merging. The calculated weighting scheme was $1/[\sigma^2(F_o^2) + (0.0529P)^2 + 61.9632P]$, where $P = (F_o^2 + 2F_c^2)/3$. Scattering factors are implemented in the refinement program.[56] The largest peak and hole in the difference map is 1.896 (close to one metal center) and −1.161 e Å^{-3}. Crystallographic data for **2** are given in Table 5.

EHMO Calculations. Calculations of the extended Hückel type[24] were carried out using a modified version of the Wolfsberg—Helmholtz formula.[57] The investigated compound was modeled using the geometrical parameters obtained from the reported crystal structure. Calculations were made with the program CACAO,[58] and the atomic parameters used are those implemented in this program.

Table 5. Crystallographic Data for 2

compound	$[Ir_2(\mu\text{-H})(\mu\text{-Pz})_2H_3(NCCH_3)(P^iPr_3)_2]$
chem formula	$C_{26}H_{55}Ir_2N_5P_2$
fw	884.09
temp, K	150.0(2)
cryst syst	monoclinic
space group	$P2_1/c$ (no 14)
a, Å	15.736(4)
b, Å	13.150(3)
c, Å	15.746(4)
β, deg	101.29(2)
V, Å^3	3195(2)
Z	4
ρ(calcd), g cm^{-3}	1.838
μ, mm^{-1}	8.444
θ range data collect, deg	2.0−24.0
index ranges	$-1 \le h \le 17$, $-14 \le k \le 15$, $-18 \le l \le 17$
no. of colld reflns	7801
no. of unique reflns	4587 ($R_{int} = 0.0687$)
abs corr method	ψ-scan[54]
min, max transmssn factors	0.295, 0.748
data/restraints/param	4259/100/316
$R(F)$ [$F^2 > 2\sigma(F^2)$][a]	0.0670
w$R(F^2)$ [all data][b]	0.1752
S [all data][c]	1.030

[a] $R(F) = \sum||F_o| - |F_c||/\sum|F_o|$, for 2893 observed reflections. [b] w$R(F^2) = (\sum[w(F_o2 - F_c2)^2]/\sum[w(F_o2)^2])^{1/2}$. [c] $S = [\sum[w(F_o2 - F_c2)^2]/(n - p)]^{1/2}$; n = number of reflections, p = number of parameters.

Acknowledgment. This work received financial support from the Spanish "Dirección General de Investigación Científica y Técnica" (DGICYT) (Project Nos. PB94-1186 and PB95-0318). V.I.B. thanks Iberdrola Company for an Iberdrola Visiting Professorship. L.A.O. thanks the Alexander von Humboldt Foundation for a Research Award.

Supporting Information Available: Tables of crystal structure data, atomic coordinates, bond distances and angles, and isotropic and anisotropic displacement parameters of **2** (8 pages). Ordering information is given on any current masthead page.

OM970972O

(54) (a) *XPREP Program*, release 5.03; Siemens Analytical X.-Ray Instruments, Inc.: Madison, WI, 1994. (b) North, A. C. T.; Phillips, D. C.; Mathews, F. S. *Acta Crystallogr., Sect. A* **1968**, *24*, 351.

(55) Altomare, A.; Cascarano, G.; Giacovazzo, C.; Guagliardi, A. *J. Appl. Crystallogr.* **1994**, *27*, 435.

(56) Sheldrick, G. M. *SHELXL-93*; University of Göttingen, Göttingen, Germany, 1993.

(57) Ammeter, J. H.; Bürgi, H. B.; Thibeault, J. C.; Hoffmann, R. *J. Am. Chem. Soc.* **1978,** *100*, 3686.

(58) Mealli, C.; Proserpio, D. M. *J. Chem. Educ.* **1990**, *67*, 399.